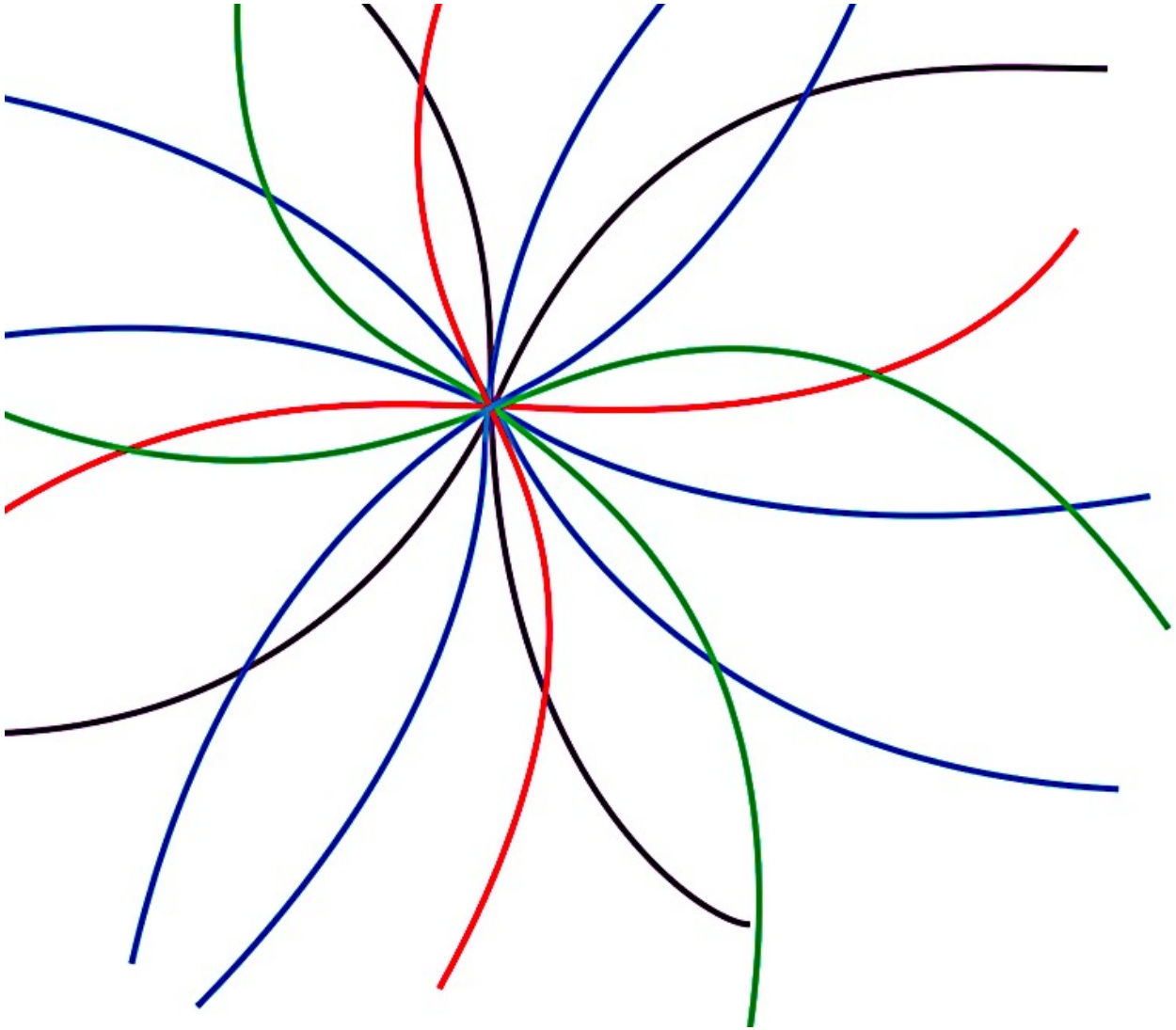

Applied research with heavy ion beams

Oleg Belov

Veksler and Baldin Laboratory of High Energy Physics
Joint Institute for Nuclear Research
E-mail: oleg.belov@jinr.int

NICA Days 2023
2 – 3 October 2023, Belgrade, Serbia

Outline

I. Basics on interaction of heavy ions with matter

II. Applied research with NICA ion beams

III. Sample activities and selected results

IV. Ways to be involved in the ARIADNA collaboration on applied research at NICA

Natural and artificial sources of heavy ions

Space radiation

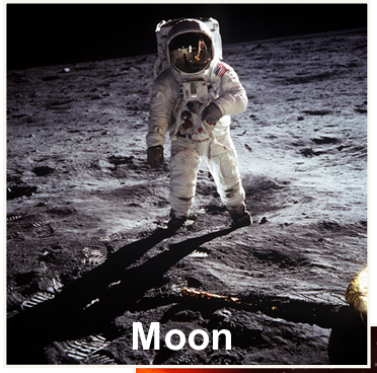

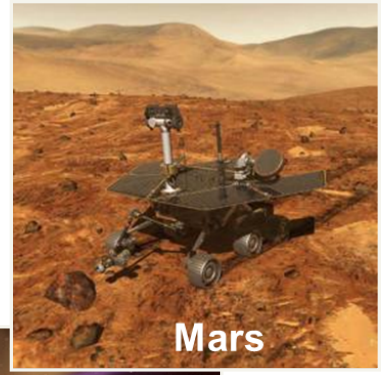

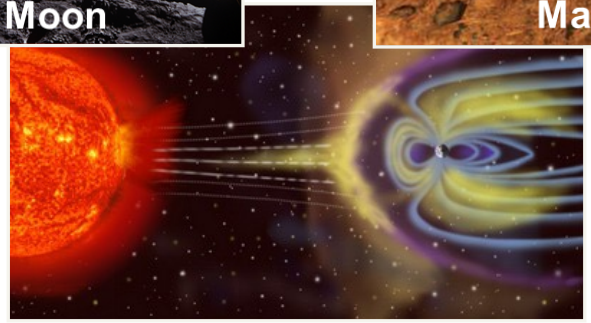

Particle accelerators

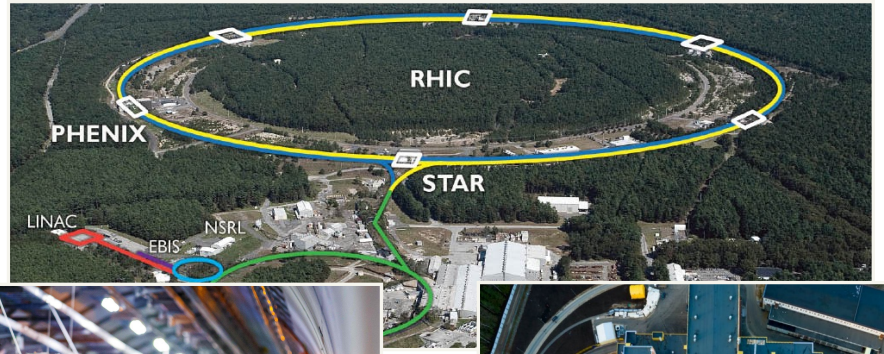

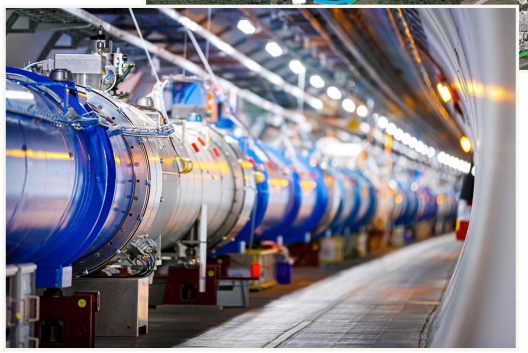

HEAVY IONS: INTERACTION WITH MATTER

In many solids heavy ions release sufficient energy to induce permanently modified cylindrical zones, so-called ion tracks.

In biological matter heavy ions leave a trace of damage to biomolecules and induce a cascade of water and organic radiolytic specie production, which evolves with time.

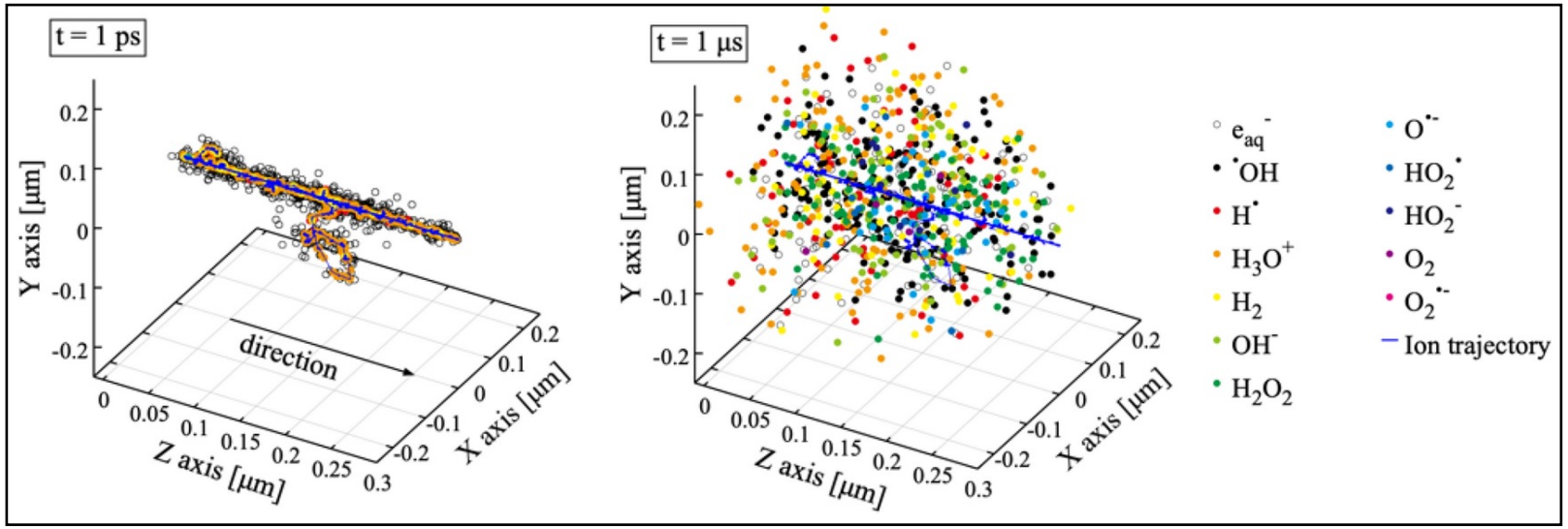

Chemical evolution of 400 MeV/u carbon ion track in water in the time 1 ps to 1 µs (Baba, K., Kusumoto, T., Okada, S. *et al. Sci Rep* 11, 1524, 2021)

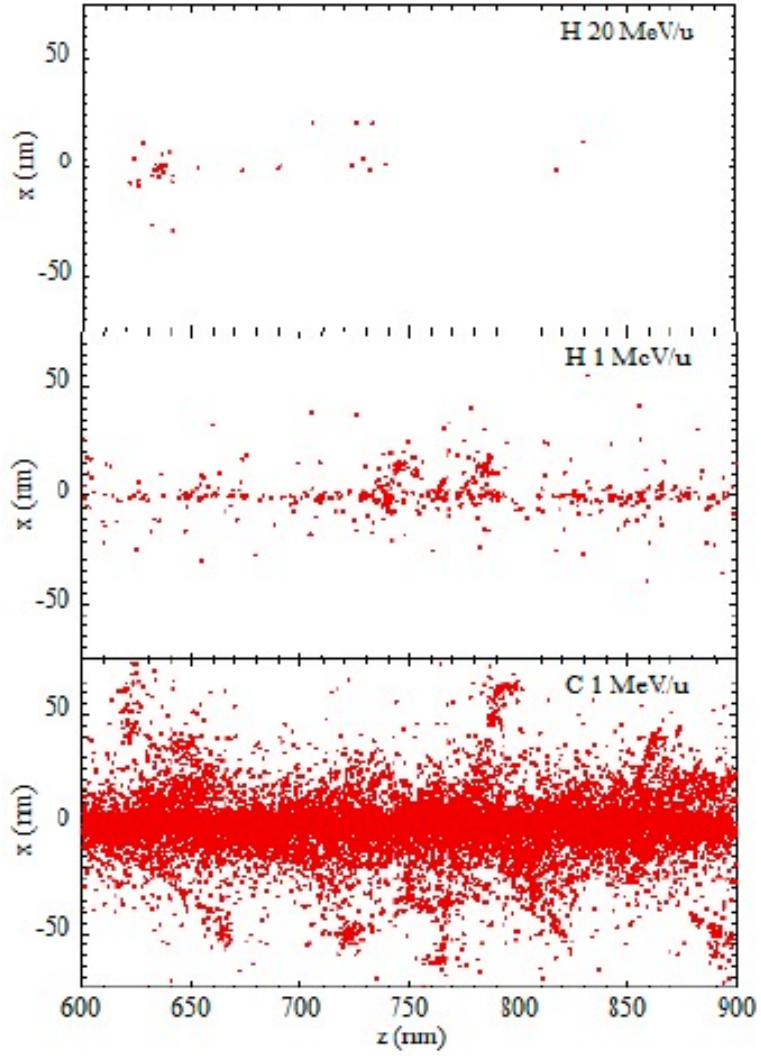

Y. Ngono-Ravache, M. Ferry, S. Esnouf, E. Balanzat. 2nd Int. Workshop Irradiation of Nuclear Materials: Flux and Dose Effects (2016)

STRUCTURE OF AN ION TRACK

Track core
Diameter ≤ 10 nm

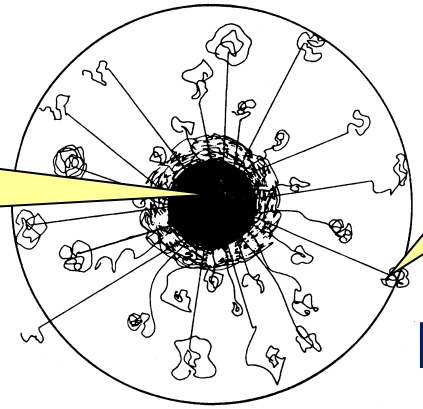

Track halo
Diameter up to ~ 100 nm

(after Chatterjee and Magee (1980))

Radial projection

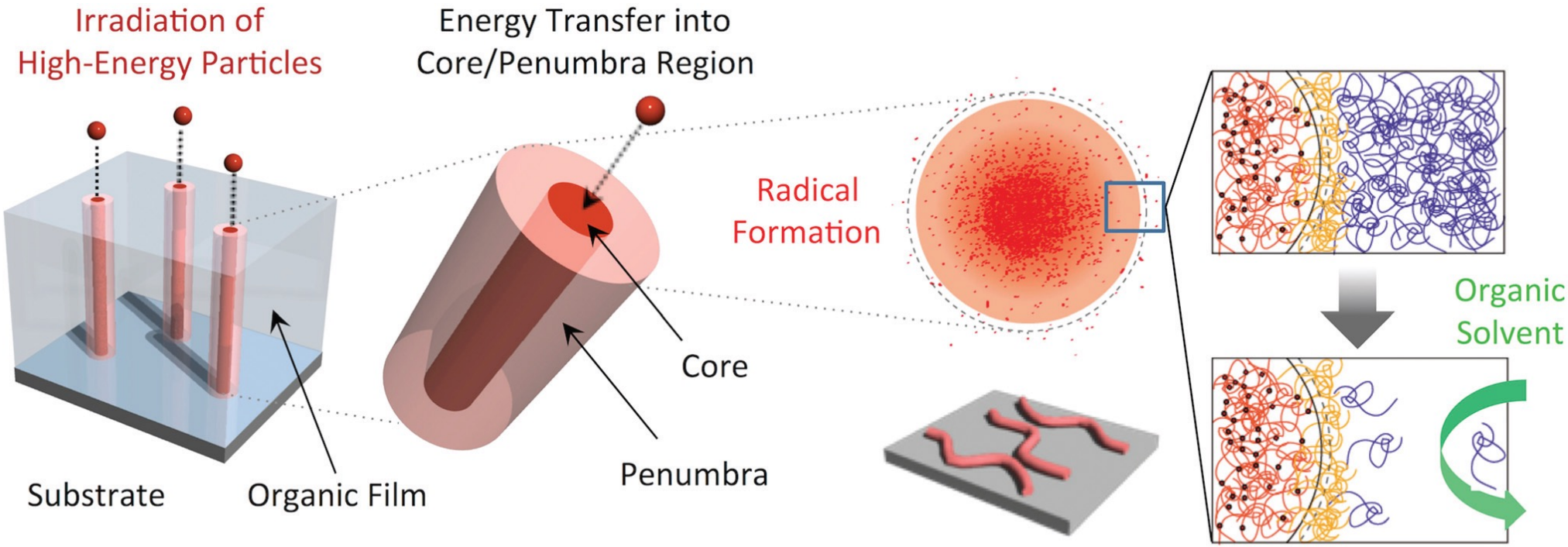

Modified from Horio A. et al. Nanoscale. 2016 8(32)

HEAVY IONS: PATTERN OF ENERGY DEPOSITION TO A MATTER

Ion beam characteristics :

✓ *Energy deposited along the path in a reduced space*

✓ *High LET*

Ion track = core + penumbra

Track: Heterogeneous

Track core: more or less homogeneous

Heavy ions = High ionization/excitation densities

Energy deposited through interactions between :

✓ the ions and target electrons

✓ the secondary electrons and the target electrons

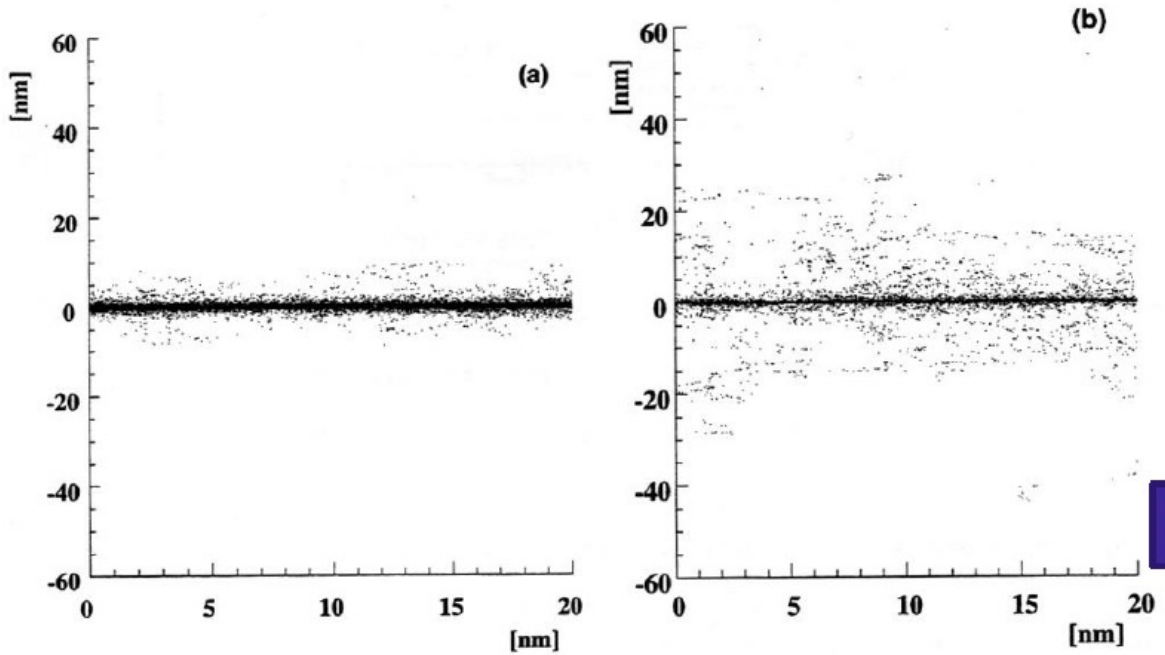

Radial distribution of dose

✓Radius ↗ when E ↗

✓$Dr_{0.5}$ ↗ when E↘

SHI = 2 Parameters (LET + $Dr_{0.5}$)

DOSIMETRY WITH HEAVY ION BEAMS: BASICS AND MAIN PROBLEMS

The conventional dosimetry operates mainly with macroscopic quantity being the **absorbed dose.**

The absorbed dose, D, is the quotient of $\mathrm{d}\bar{\varepsilon}$ by $\mathrm{d}m$, where $\mathrm{d}\bar{\varepsilon}$ is the mean energy imparted by ionizing radiation to matter of mass $\mathrm{d}m$, thus

$$D = \frac{\mathrm{d}\bar{\varepsilon}}{\mathrm{d}m}$$ */ICRU Report No. 85/*

Unit: J kg^{-1}

The special name for the unit of absorbed dose is gray (Gy).

The macroscopic dosimetry with heavy ions works nice in the case of solids but falls with small objects (biomolecules, living cells, microelectronic devices, etc.).

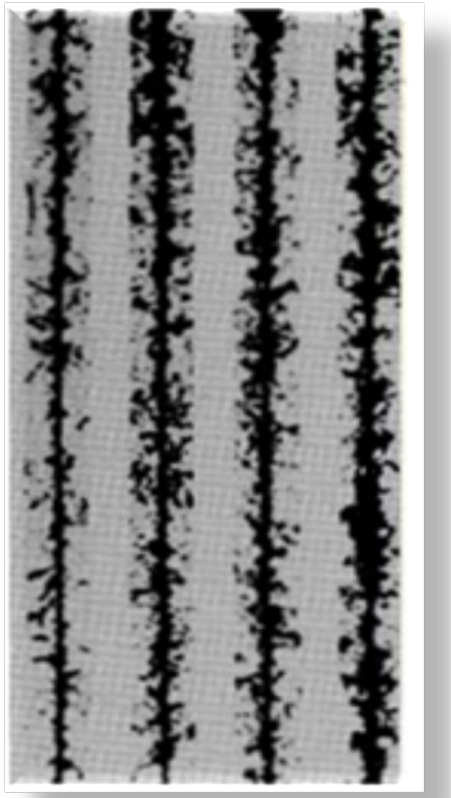

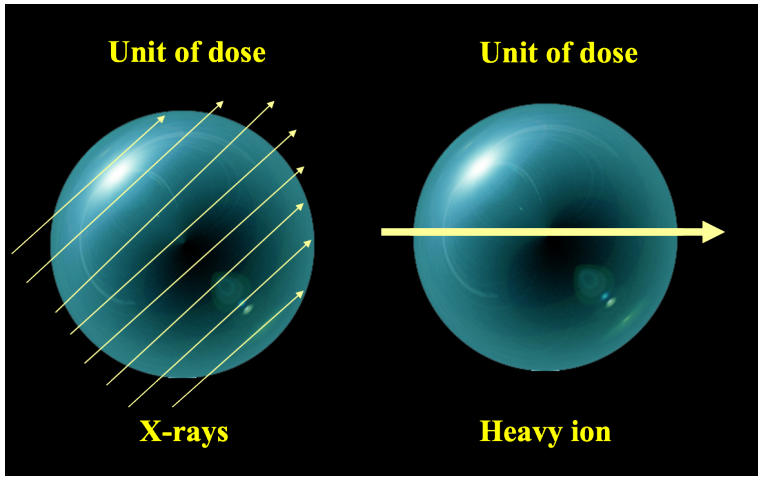

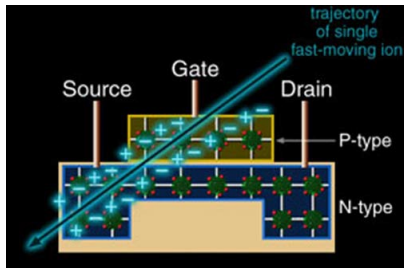

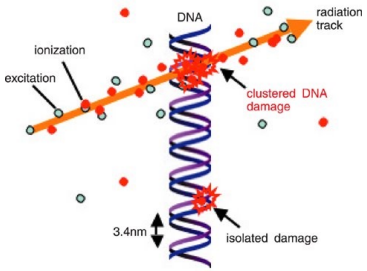

Form their very beginning, experiments with heavy ions and small targets like living cells and biomolecules have identified the problem of microdosimetry because of their stochastic nature of energy deposition.

FROM MACRODOSIMETRY TO MICRODOSIMETRY

The early **target theories** attempted to describe the discrete acts of energy transfer, termed **"hits"** identifying them with individual ionizations or clusters of ions.

The spatial correlation of these events was not considered, and target theory in this earliest form could not explain the relative biological effectiveness of different types of ionizing radiation.

Three principles of the target theory:

1. The cell has an unique target smaller than the cell and sensitive to radiation.

2. Radiation energy is transferred to the cell in a discrete way.

3. Separate acts of energy deposition occur independently.

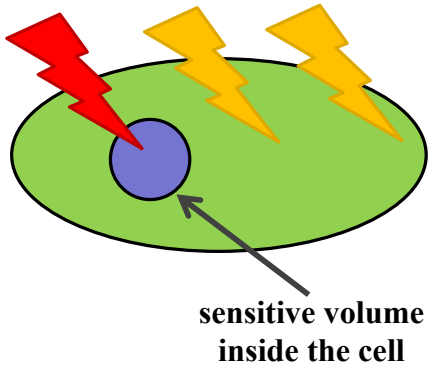

$$\bar{n} = VD$$

$$P_{(k)} = \frac{e^{-\bar{n}}\bar{n}^{k}}{k!}$$

Poisson distribution

$$P_{(0)} = e^{-VD}$$

Probability of cell survival

Later on, it was shown that the *V* parameter depends on many physical and biological factors. This fact did not allow to interprety correctly the exponential survival curves.

- Classical models
- Stochastic models
- Probabilistic models
- Repair models
- Molecular models
- Models taking into account the radiation quality

EVOLUTION OF CLASSICAL MODELS FOR CELL SURVIVAL

One more problem: the analysis of survival curves having a "shoulder"

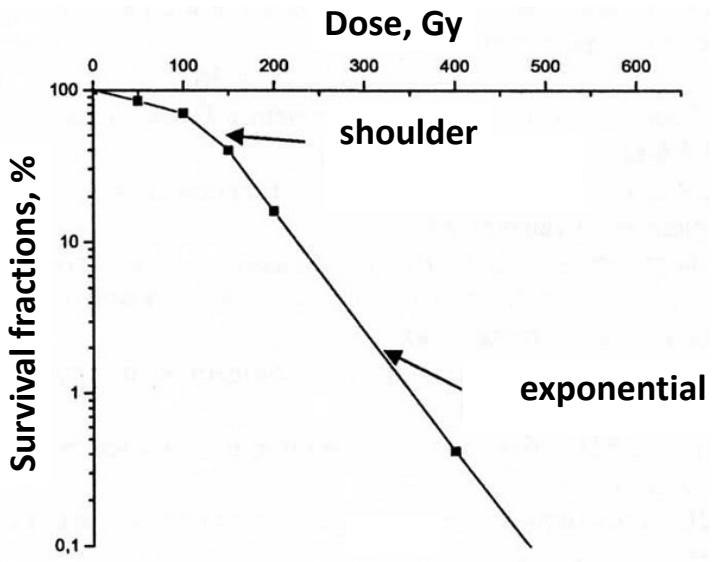

Multi-target formula: $P'_{(m)} = 1 - (1 - e^{-VD})^m$

where ***m*** is the number of targets

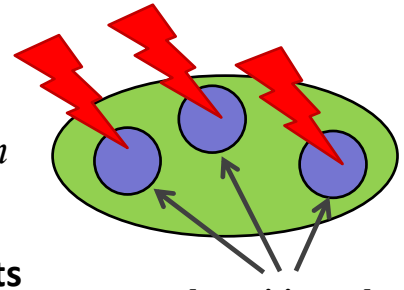

several sensitive volumes inside the cell

Multi-hit formula: $P'_{(n)} = e^{-VD} \sum_{k=0}^{n-1} \frac{(VD)^k}{k!}$

where ***n*** is the number of hits

multi-hit process

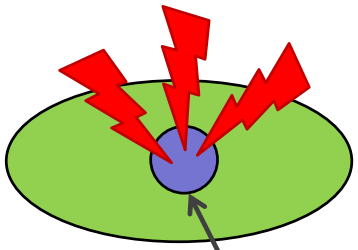

sensitive volume inside the cell

Multi-target and multi-hit formula: $P'_{(n,m)} = 1 - \left(1 - e^{-VD} \sum_{k=0}^{n-1} \frac{(VD)^k}{k!}\right)^m$

m is the number of targets, ***n*** is the number of hits

multi-target and multi-hit process

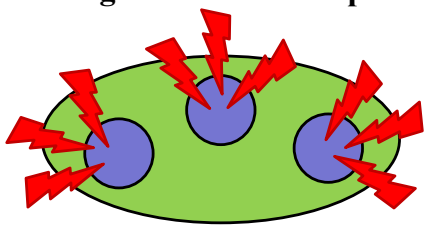

- The parameters ***m*** and ***n*** do not have a real biophysical meaning.
- These parameters vary significantly under changes of some physical and biological factors.

STOCHASTIC MODELS

Cells irradiated with the same dose have an equal probability of successful division (of survival). But as the cell division process is stochastic (depending on biological variability), cell survival is probabilistic.

Suggesting the equal number of initial lesions in cells, it is supposed that each lesion is caused by changes in the number of some cell structures. These changes lead to an increase in the failure probability during cell division.

$$-dN = S' N_0 dt$$

dN is the number of surviving cells;
N_0 is the initial number of cells;
S'(*t*, *D*) is the failure probability during cell division in the *t* unit of time.

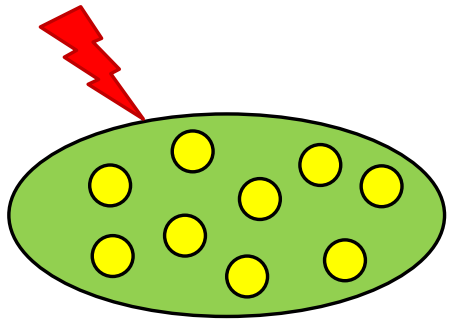

If the failure probability increases linearly with the irradiation dose $S'(t, D) = S_1'(t)D$

Then an exponential curve can be obtained:

$$N = N_0 e^{-D\int_0^{\infty} S_1'(t)dt}$$

To take into account the **target theory,** a vector is introduced, which characterizes a cell population: $\xi = (\xi_1, \xi_2, \ldots, \xi_n)$.

The initial state corresponds to $\xi_0 = (1, 0, \ldots, 0)$. Under the irradiation of the cell population *ξ* with the dose d*D*, this population transforms into a new state $\xi + d\xi = \xi + A\xi dD$, where *A* is a matrix of transition probabilities of the *n* × *n* order. The solution of this equation is $\xi = \xi_0 e^{AD}$.

If we suppose that cells in state *n* – 1 are able to repair the damage and in the state *n* they die, then the survival curve can be described as

$$S = \sum_{k=1}^{n-1} \xi_k .$$

The main problem with the stochastic models is the assumption on the same vulnerability of cells exposed to same dose.

PROBABILISTIC MODELS

Probabilistic models combine the target theory and biological stochastics.

Let us put $\alpha < 1$ which is the probability of a failure in cell division (the probability of cell death), and $P_1 = 1 - \alpha$ is the probability of successful cell division (survival). Then, this probability for cells with i lesions will be

$$P_i = (1-\alpha)^i$$

(based on the assumption that all lesions are independent on each other).

Cell survival is described as $$S = \sum_{i=0}^{k} \frac{e^{-a} a^i}{i!} \left(1 - \left(\frac{1-(1-\alpha)^i}{(1-\alpha)^i}\right)^2\right)$$

Here b is the probability of lesion formation per unit dose;

$a = bD$ is the average number of lesions;

k is the number of lesions when $(1-\alpha)^k > 0.5 \geq (1-\alpha)^{k+1}$.

The curves calculated using probabilistic models are superpositions of several multi-hit curves with the critical number of hits from 0 to *k*.

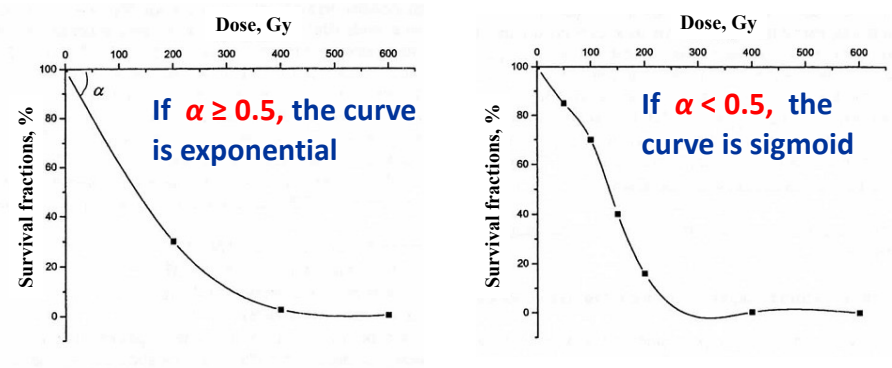

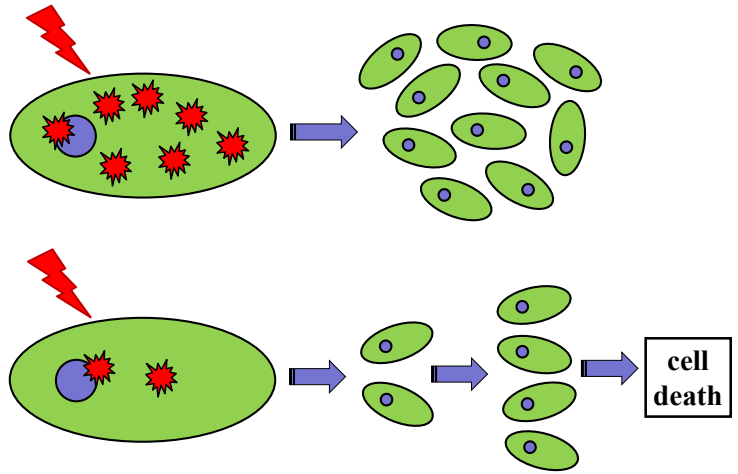

Probabilistic models can reconstruct different types of survival curves and explain some effects of irradiation. But they do not take into account the possibility of damage repair, which determines the different outcomes.

REPAIR MODELS

The cell inactivation caused by radiation is connected with the repair process.

$$S = e^{-kD+\alpha\left(1-e^{-\beta D}\right)}$$

kD is the number of cell lesions (proportional to the dose D);

$\alpha\,(1 - e^{-\beta D})$ is the number of repaired lesions;

α is the probability of a failure in cell division (probability of cell death);

β is the probability of damage repair per unit dose.

The repair models described the induction and elimination of lesions only formally and did not take into account real intracellular biophysical mechanisms.

Each target can be in two states

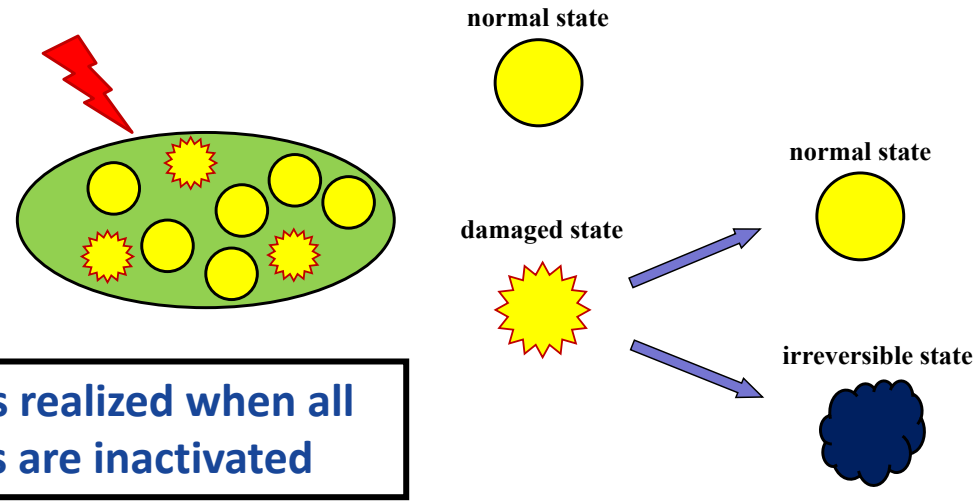

Cell death is realized when all such targets are inactivated

MOLECULAR MODELS

Molecular models assumes a dependence of the cell survival on the position of radiation-induced damage at the DNA molecule.

The lethal outcome for the cell is the induction of a straight double-strand DNA break or two overlapping single-strand DNA breaks.

$$S = e^{-\alpha D - \beta D^2}$$

α is the probability of the induction of a straight double-strand break;

β is the probability of the induction of a double-strand break from two overlapping single-strand breaks.

$$S = e^{-N\beta D}\left(1 - e^{-\frac{l_0 \beta D}{M}}\right)$$

β is the yield of the initial DNA lesions; l_0 is the size of a DNA gap; M is the genome size; N is the factor of the nearest non-simultaneous lesions in the opposite DNA strands.

Such curves have a small shoulder in the low-dose region and an exponential part at the high levels of irradiation.

Single-strand DNA break

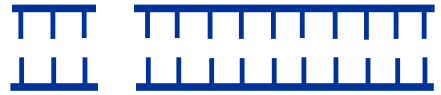

Straight double-strand DNA break

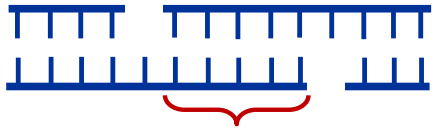

Double-strand break produced by the overlapping of two single-strand ones

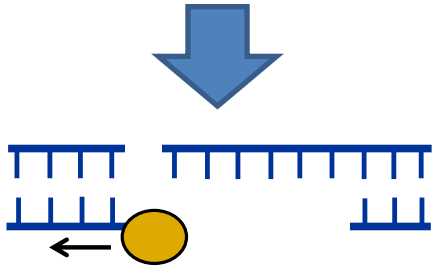

Double-strand break produced by the enzymatic degradation of DNA

MODELS TAKING INTO ACCOUNT THE RADIATION QUALITY

More realistic models were proposed through a more detailed description of the "random" configurations of energy deposition in the tracks of charged particles.

The term "Linear Energy Transfer" or LET was introduced to characterize how a particle loses energy along its track. The LET basically determines the radiation quality.

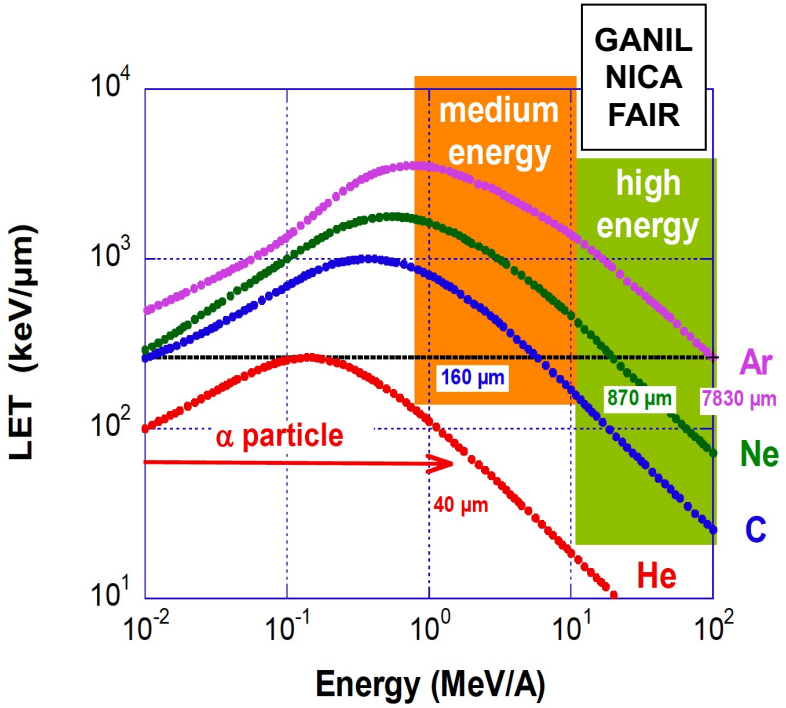

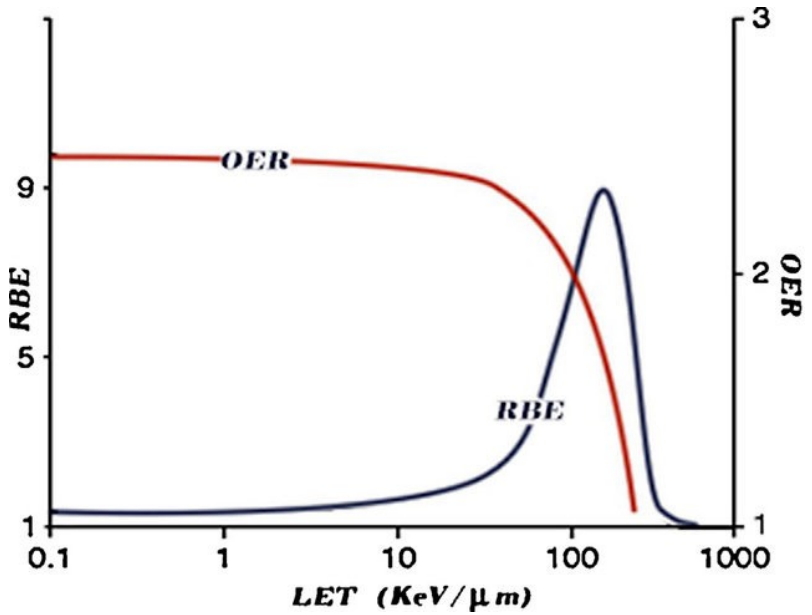

Linear energy transfer

$$L = \frac{\mathrm{d}E}{\mathrm{d}x}$$

The energy d*E* lost per unit length d*x* of particle track in the matter.

Unit: keV/µm

In **microdosimetry** one is interested in measuring or estimating the **distribution of energy transfer along a particle's track.**

Therefore the quantities used in microdosimetry are somewhat different than those used in conventional dosimetry.

When a small sensitive target (i.e. cell nucleus) is exposed to heavy ions, the morphologically complicate structure is combined with a complicate pattern of energy deposition.

The best-known example is radiation damage to DNA.

Cell nucleus has a complicate morphology structure. Each chromosome occupies the exact chromosome territory.

DNA is very tightly folded, it is compacted in a way that allows it to easily become available to the many enzymes

416 MeV/n Fe ion track + DSB

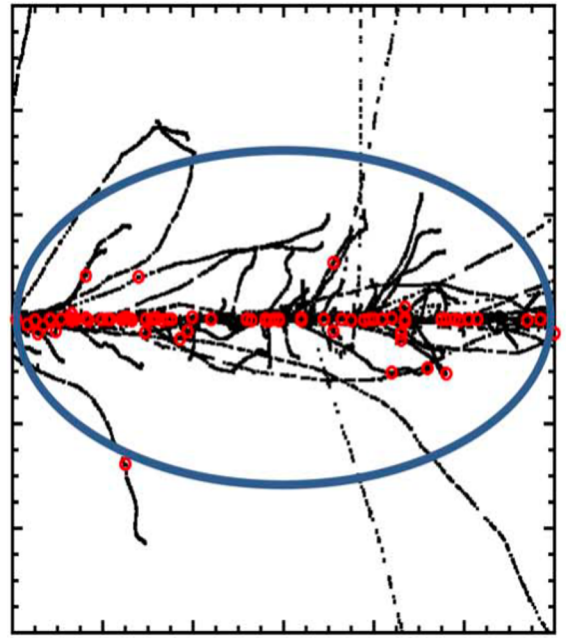

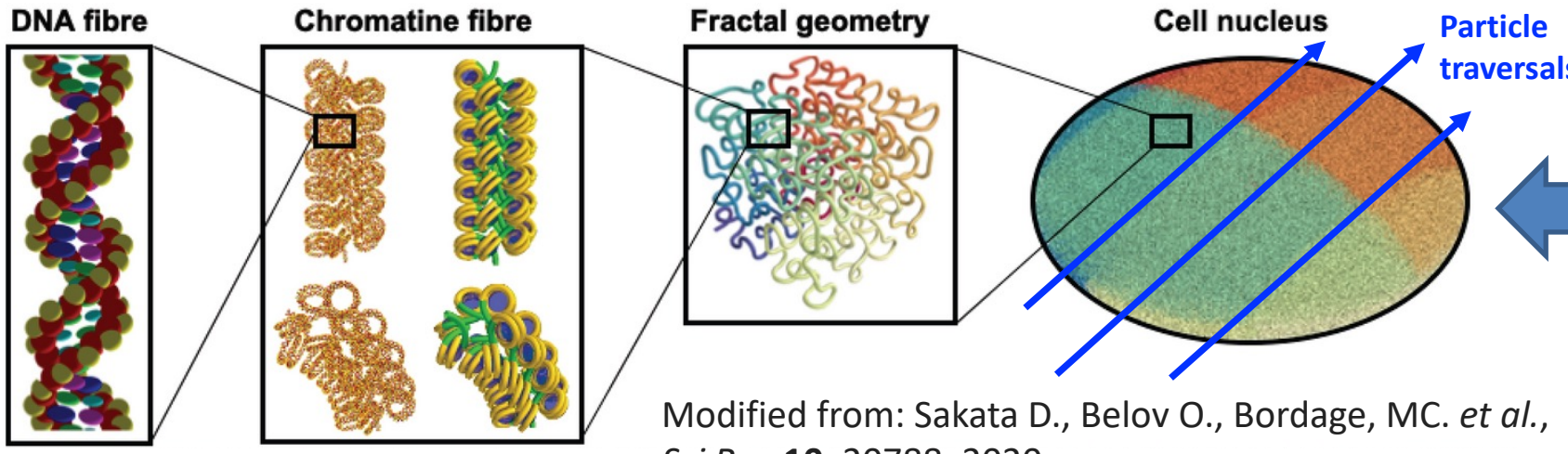

Modified from: Sakata D., Belov O., Bordage, MC. *et al.*, *Sci Rep* **10**, 20788, 2020

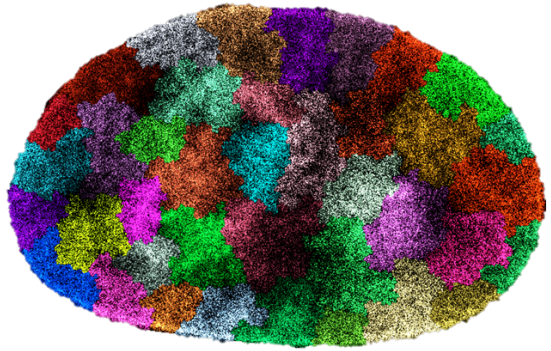

Chromosome territories (nucleus). Measurements by Kirti Prakash (Rowitch lab)

Nevertheless, pattern of energy deposition exhibited by heavy ions has some practical benefits.

- In radiation modification of materials: there is an option to induce precise radiation defects (latent tracks), which then can be transformed into the pores with different parameters.
- In radiation medicine, ion therapy demonstrates a more precise shape around the solid tumors than sparsely ionizing radiation and even more precise than proton therapy.

Variety of pore shapes in track-etched membranes

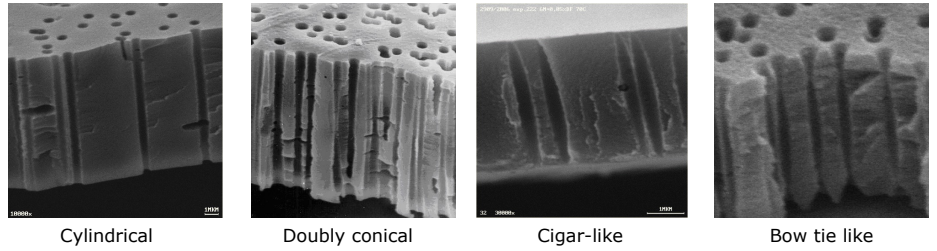

Cylindrical | Doubly conical | Cigar-like | Bow tie like

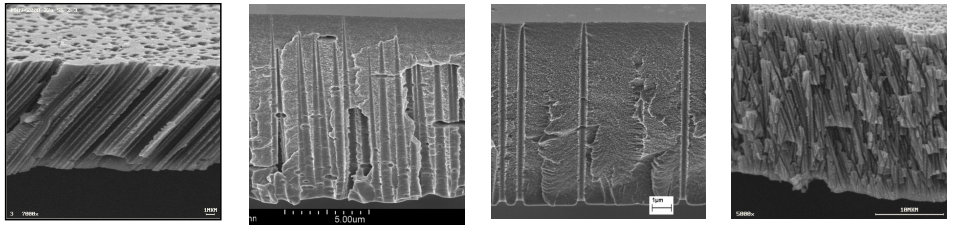

Cylindrical, parallel, all tilted at an angle of 45° | Conical | Highly asymmetric with bullet-like tip | Cylindrical, non-parallel (typical commercial membrane for microfiltration)

D. Schulz-Ertner, H. Tsujii. J.Clin. Oncol. 2007

P. Apel. 2021. Applied Research @ NICA meeting

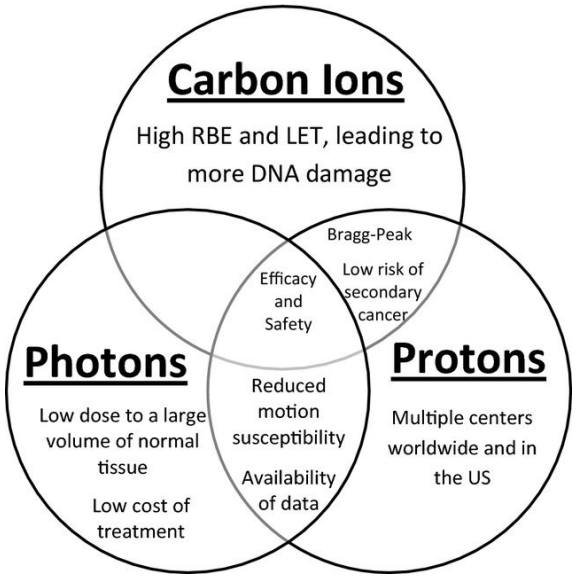

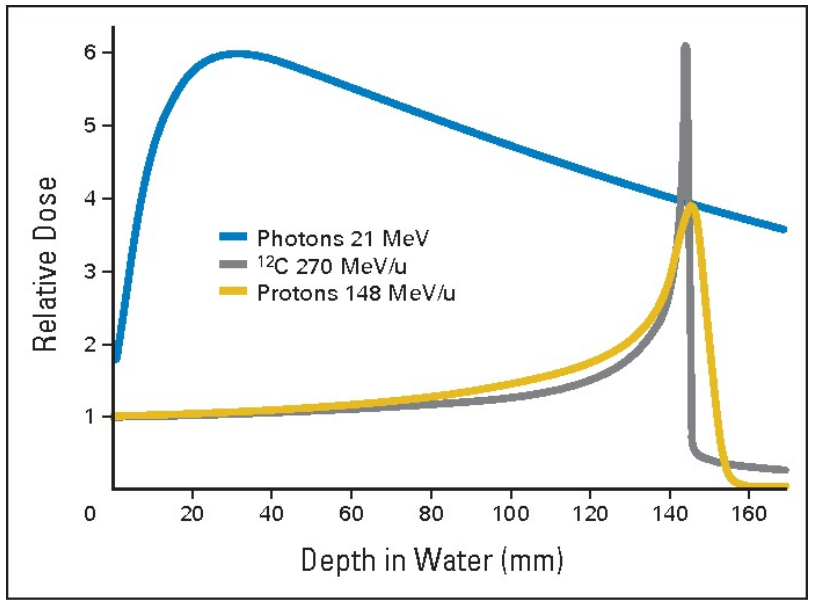

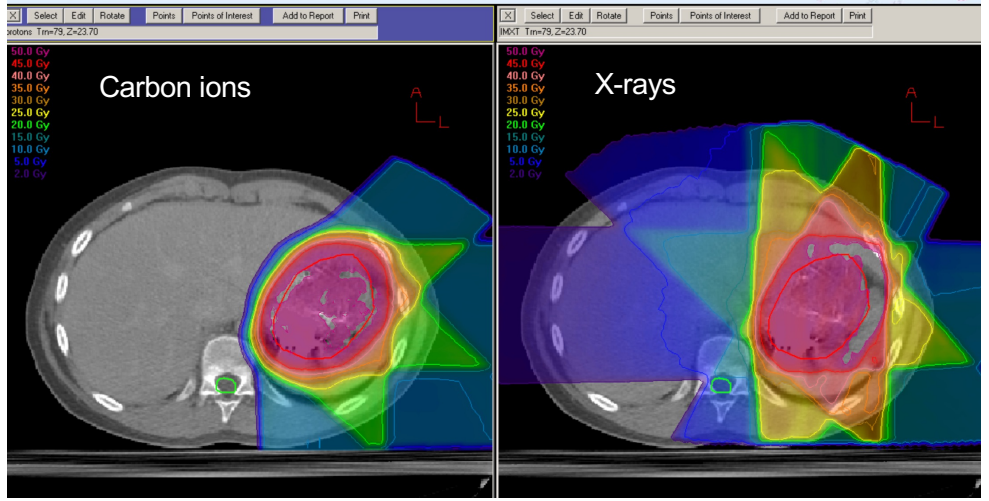

Jiade J. Lu et al. IAEA Scientific Forum, 2017

II. Applied research with NICA ion beams

NICA FACILITIES FOR APPLIED RESEARCH

The Applied Research Infrastructure for Advanced Developments at NICA fAcility (ARIADNA)

ARIADNA
beamlines

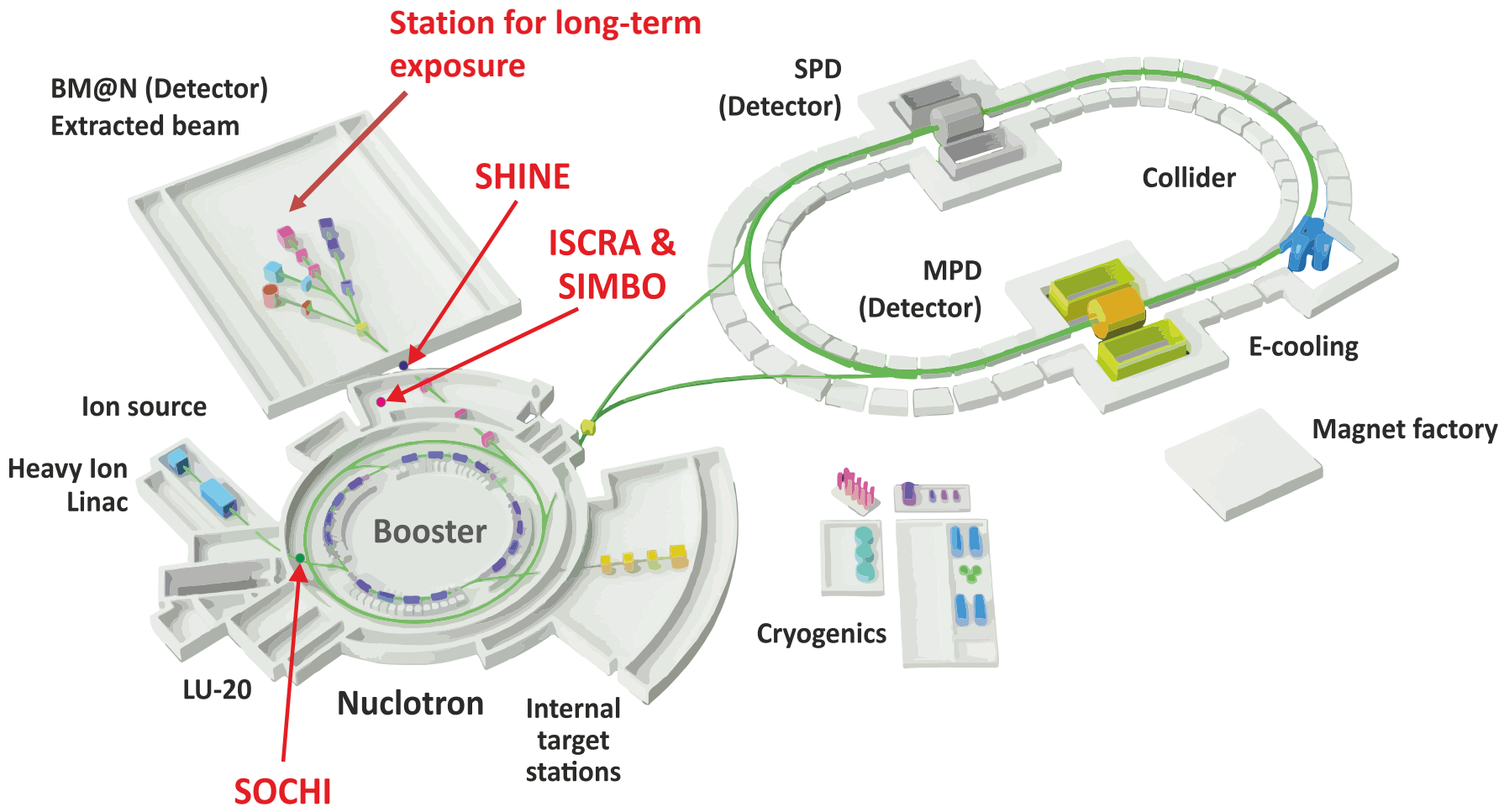

APPLIED RESEARCH @ NICA

The Applied Research Infrastructure for Advanced Developments at NICA fAcility (ARIADNA) will include:

(1) Beamlines with magnetic optics, power supplies, beam diagnostics systems, cooling systems, etc.

(2) Experimental zones equipped with target stations for users (detectors, sample holders, irradiation control and monitoring system, etc.)

(3) Supporting user infrastructure (areas for deployment of user's equipment, for sample preparation and post-irradiation express analyses, etc.)

Low-energy ion beams available at HILAC	Intermediate-energy ion beams available at Nuclotron	High-energy ion beams available at Nuclotron
3.2 MeV/nucleon	150-1000 MeV/nucleon	up to 4.5 GeV/nucleon
Life sciences, Radiation damage to microelectronics, Materials science, Novel relativistic nuclear technology		
Protons and ions with Z = 2 to 92 Irradiation of decapsulated microcircuits and solid materials with 3.2 MeV/nucleon ions.	**Ions: $^{12}C^{6+}$, $^{40}Ar^{18+}$, $^{56}Fe^{26+}$, $^{84}Kr^{36+}$, $^{131}Xe^{54+}$, $^{197}Au^{79}$** Irradiation of capsulated microcircuits with 150-350 MeV/nucleon ions. Ions like $^{197}Au^{79+}$ are decelerated in the capsule to 5-10 MeV/nucleon. 500-1000 MeV/nucleon ions be available at the target station for biological sample irradiation.	**Ions: $^{1}H^{1+}$, $^{2}D^{1+}$, $^{12}C^{6+}$, $^{40}Ar^{18+}$, $^{7}Li^{3+}$** Target station will be equipped with targets from C to Pb and with the systems of beam and target diagnostics, positioning, thermometry, synchronization, radiation control, and data acquisition.

ARIADNA RESEARCH INFRASTRUCTURE:

CURRENT STATE AND RECENT DEVELOPMENTS

The progress was recently made in development of the NICA target stations for applied research.

In December 2021, the beamline and **Station Of CHip Irradiation (SOCHI)** was completed.

In December 2022, the **prototype of the Target station for long-term exposure with high energy ions** was assembled at the outgoing beam available behind the BM@N facility. This target station has an advantage to use beams for applied research purposes in parallel with operation of the BM@N setup.

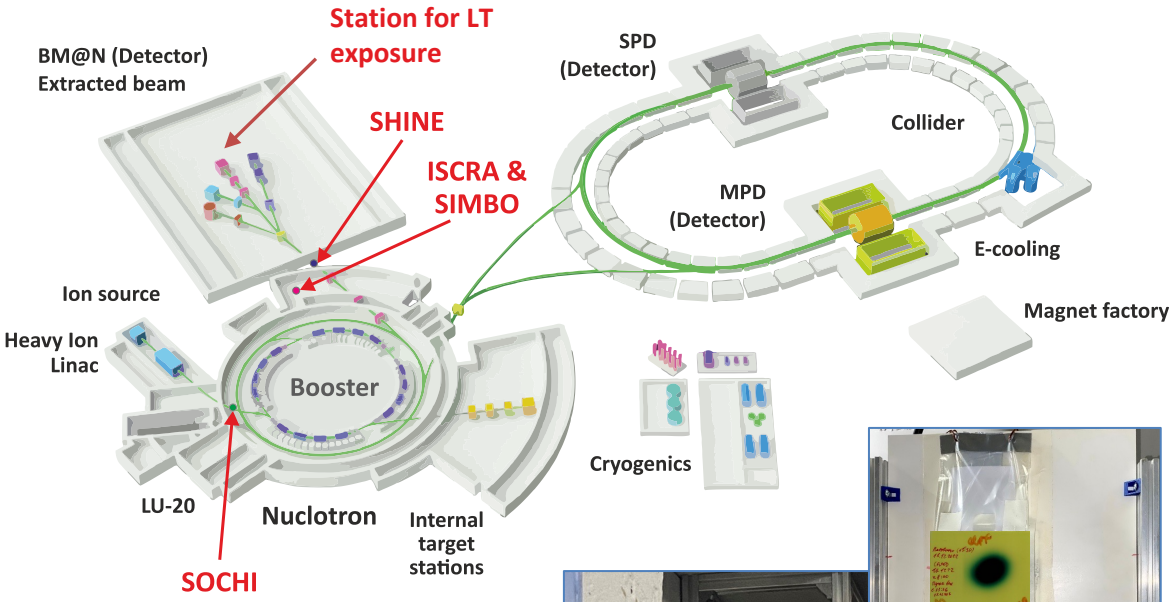

Other ARIADNA beamlines for applied research are in progress

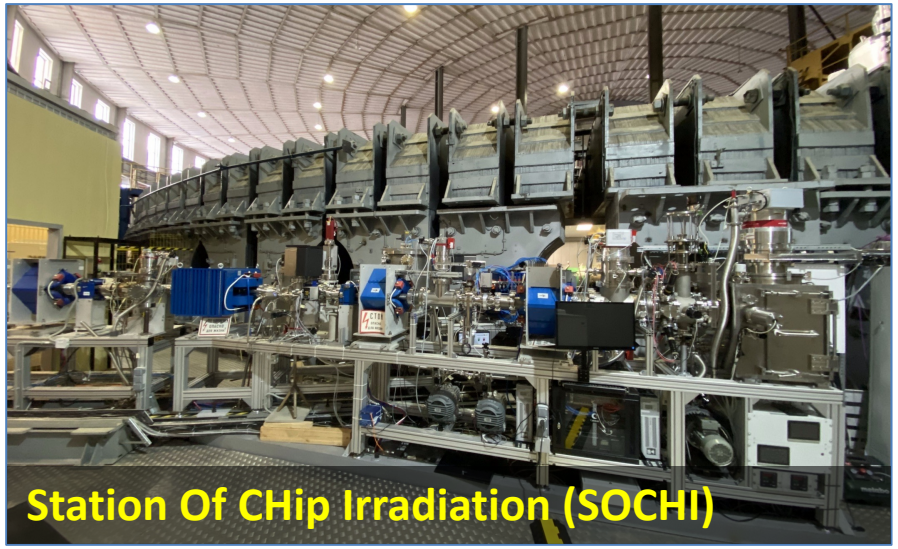
Station Of CHip Irradiation (SOCHI)


SIMBO and ISCRA target stations

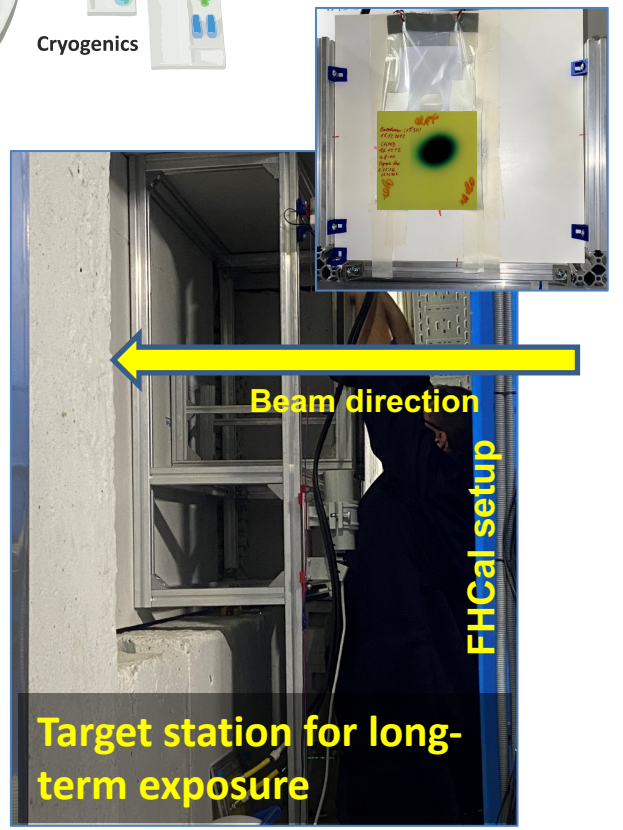

Target station for long-term exposure

LOW-ENERGY TARGET STATION FOR TESTING OF DECAPSULATED MICROELECTRONIC COMPONENTS

Low-energy beams extracted from the HILAC at energy 3.2 MeV/n.

Protons and ions Z = 2 to 92.

The beamlines ands with a vacuum chamber designed for placement and online diagnostics of the microelectronic components' state.

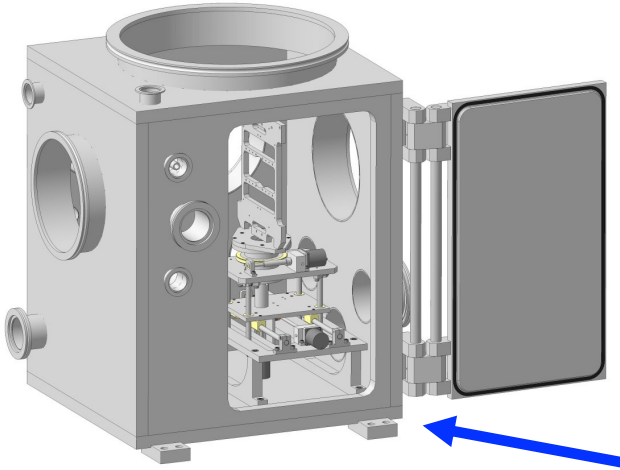

Vacuum chamber

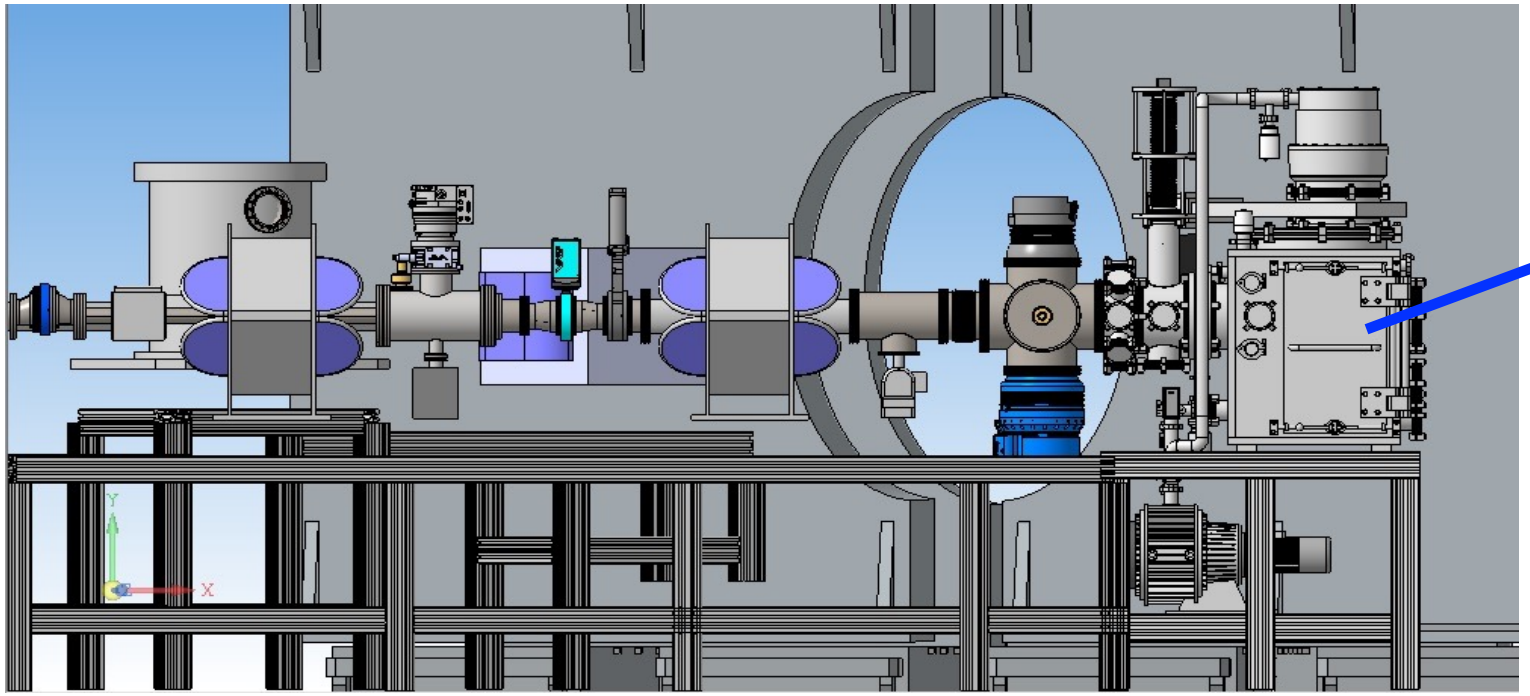

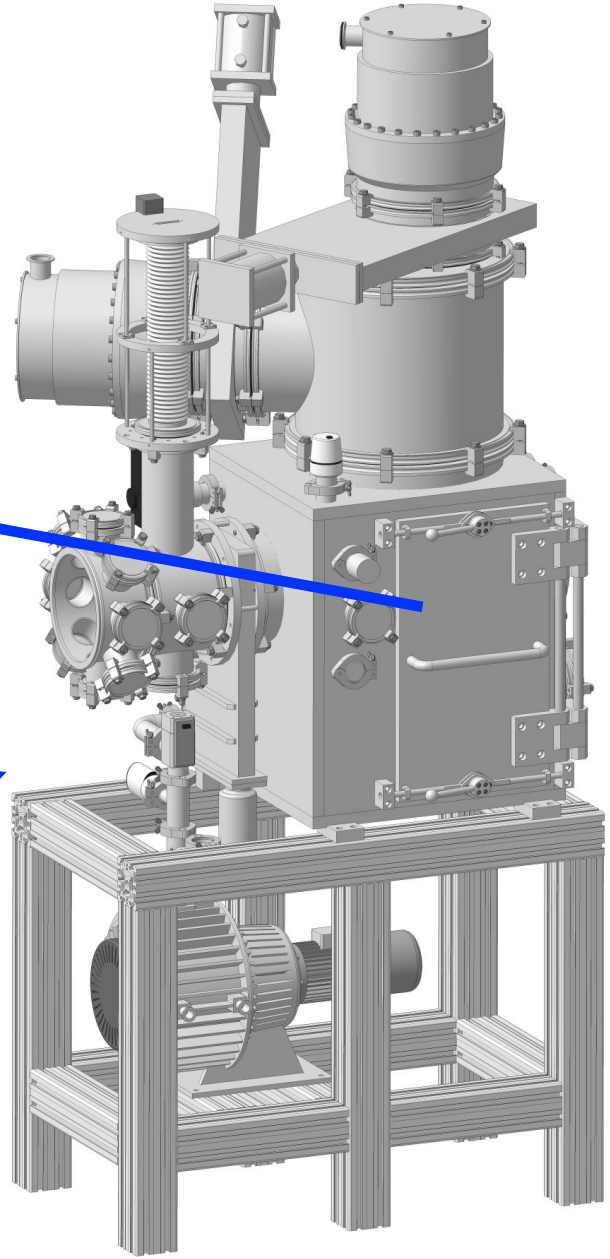

E. Syresin et al.

SOCHI FACILITY: TEST EXPERIMENT WITH IRRADIATION OF TRM-PTFE FILMS

TRM-PTFE films of 20 and 100 μm

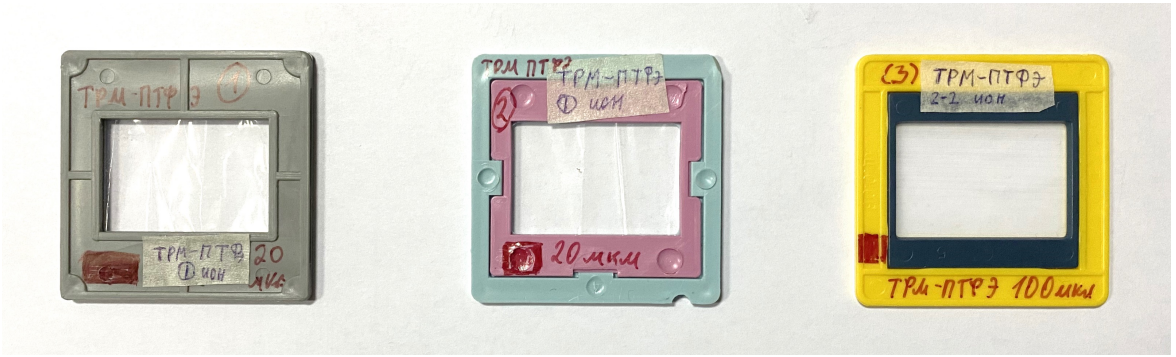

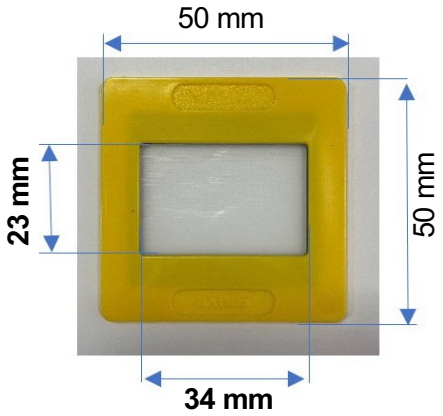

Formula: $(C_2F4)_n$

Density TRM-PTFE: 2.20 g/cm^3

Irradiation area at the film: 23 x 34 mm

EXPOSURE TO 3,2 MEV/NUCLEON $^{124}Xe^{54+}$ IONS

Irradiation in a vacuum chamber

Sample # 1 (20 μm): Φ = 1.08 x 10^6 particles/cm^2

Sample # 2 (20 μm): Φ = 1.12 x 10^5 particles/cm^2

Sample # 3 (100 μm): Φ = 1.08 x 10^6 particles/cm^2

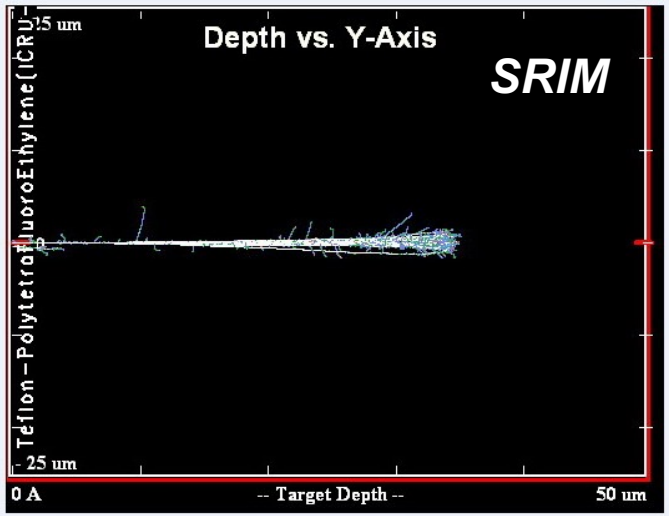

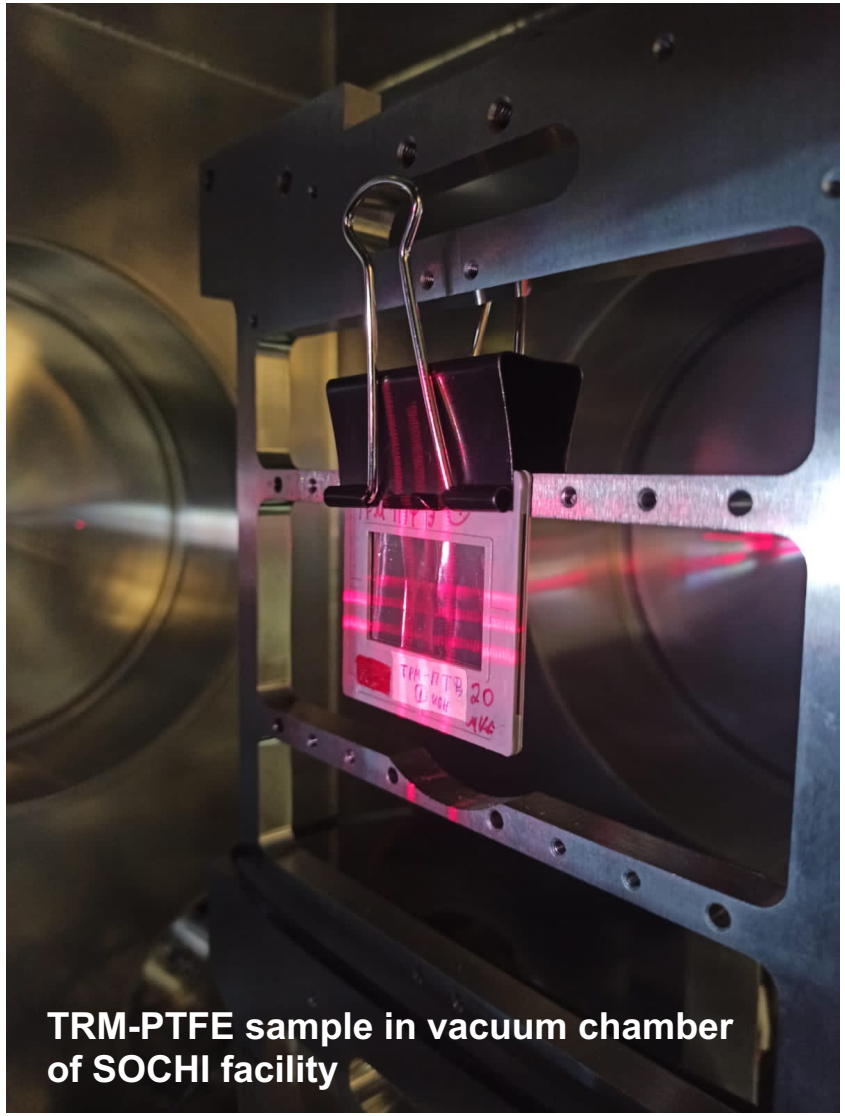
TRM-PTFE sample in vacuum chamber of SOCHI facility

High-energy target station for long-term exposure (at the BM@N facility)

First high-energy beam for applied research at NICA

First run of the target station: 11 December 2022 – 30 January 2023

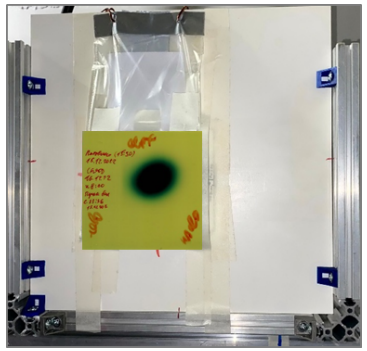

$^{124}Xe^{54+}$

3.8 GeV/nucleon

Beam trace at the EBT3 film

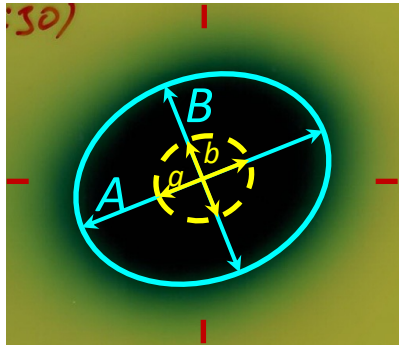

Beam parameters:
A = 34.2 mm,
B = 29.3 mm.
The most uniform area:
a = 12 mm,
b = 9 mm

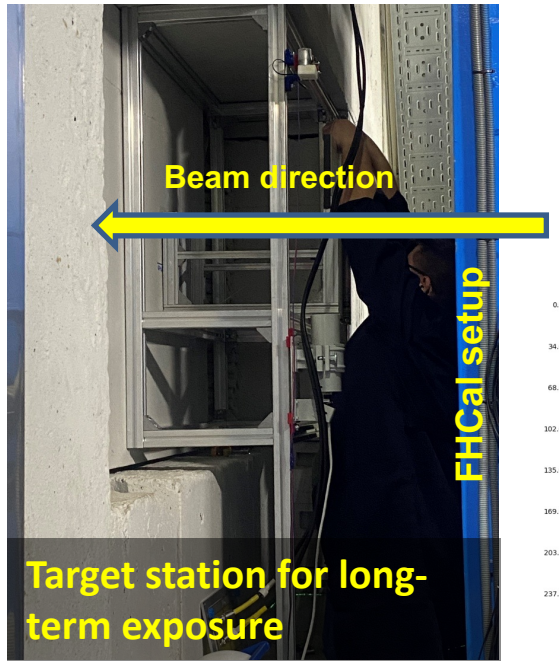

3D-map of exposure

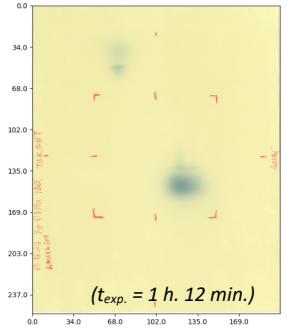

Beam profile (EBT3 film)

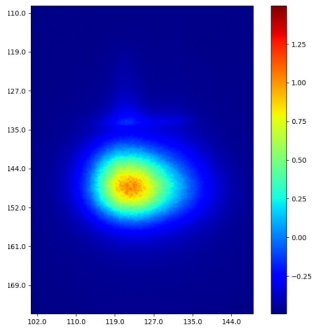

Beam profile (OCTAVIUS Detector 1500 XDR)

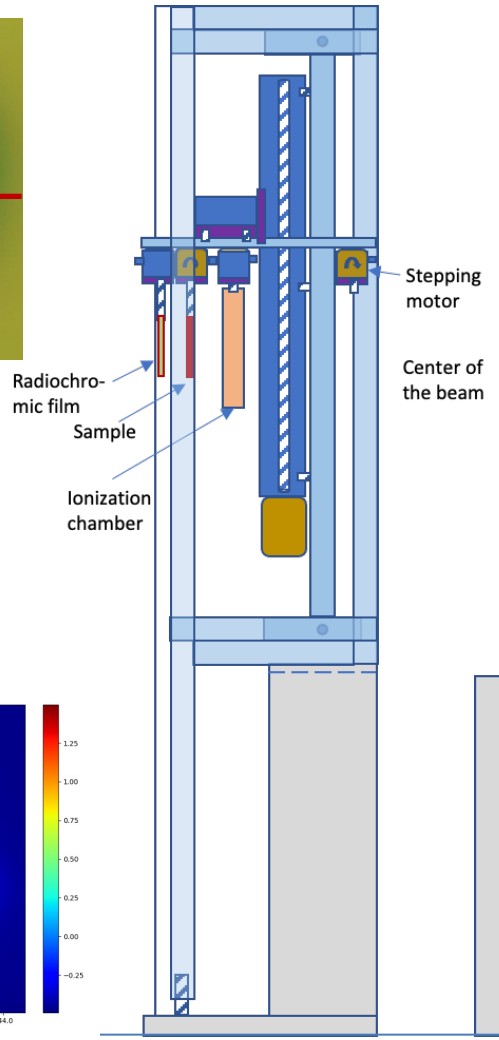

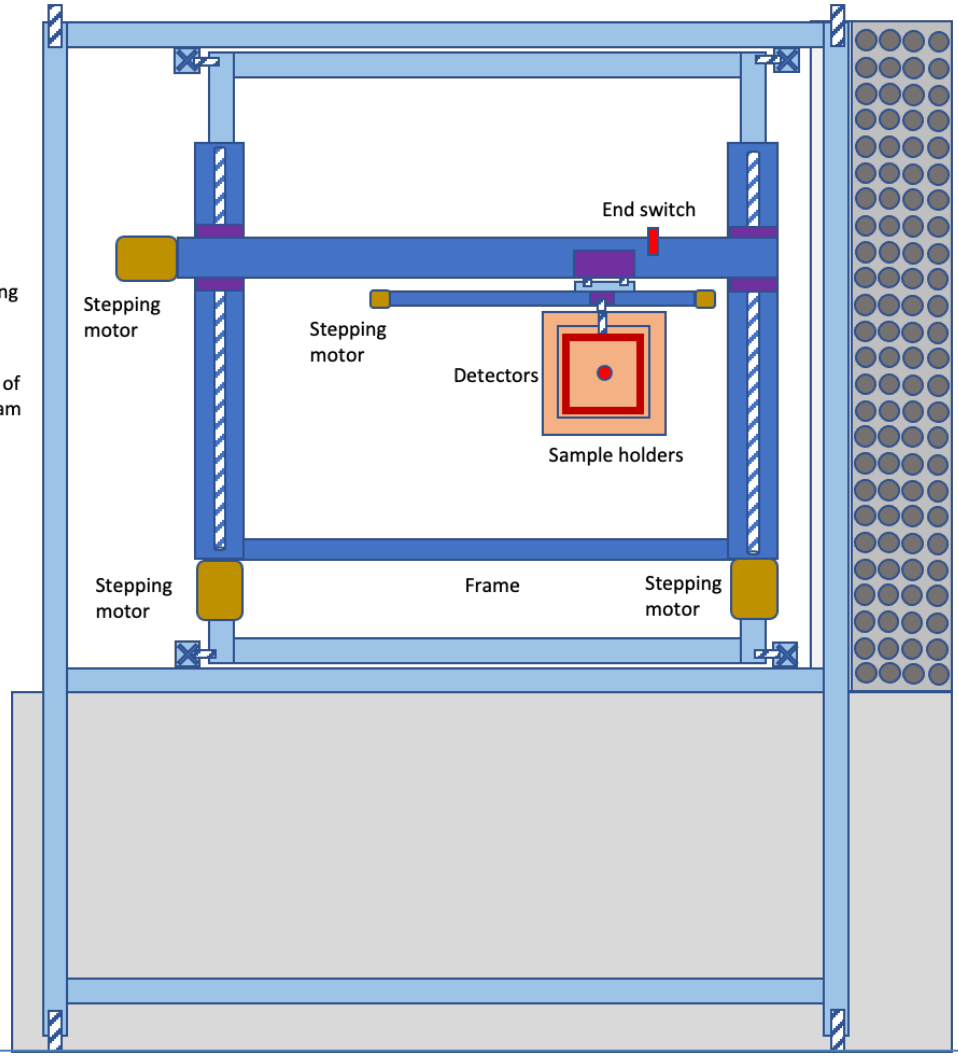

O. Belov et al.

TARGET STATION FOR TESTING OF CAPSULATED MICROELECTRONIC COMPONENTS (ISCRA)

The beam diagnostic provides measurements of ion beam profiles, primary ion fluence, the primary ion density flux, the secondary particle density flux, the radiation dose: (three ionization chambers, scintillation-fiber detector, semiconductor detector, multi electrode cylinder Faraday, Si strip detector for individual ion detection, four on-line control scintillation detectors)

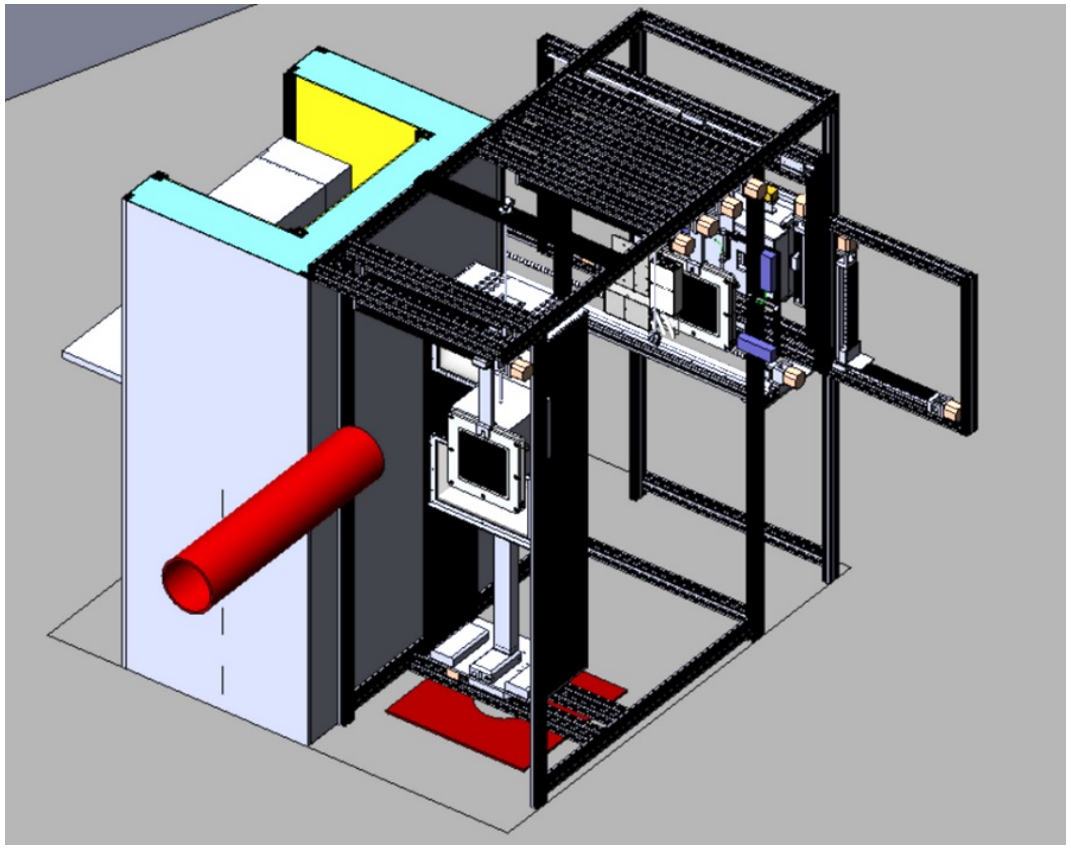

E. Syresin et al.

Beam parameters	
Ion types	$^{12}C^{6+}$, $^{40}Ar^{18+}$, $^{56}Fe^{26+}$, $^{84}Kr^{36+}$, $^{131}Xe^{54+}$, $^{197}Au^{79}$
Ion energy, MeV/n	150-350
Ion flux density, particle/(cm^2·s)	10^2 .. 1×10^5
Fluence per session, ion/(cm^2)	10^7
Area of chip irradiation of 20×20 mm without scanning, mm	∅30
Flow uniformity at chip irradiation of 20×20 mm without scanning	10%
Exposure area in scan mode, mm	200×200
Flux uniformity at scan irradiation	±15%
FWHM beam diameter at target, mm	25-73
Range of LET (Si)	1…70 MeV·cm^2/mg

TARGET STATION FOR BIOLOGICAL OBJECTS (SIMBO)

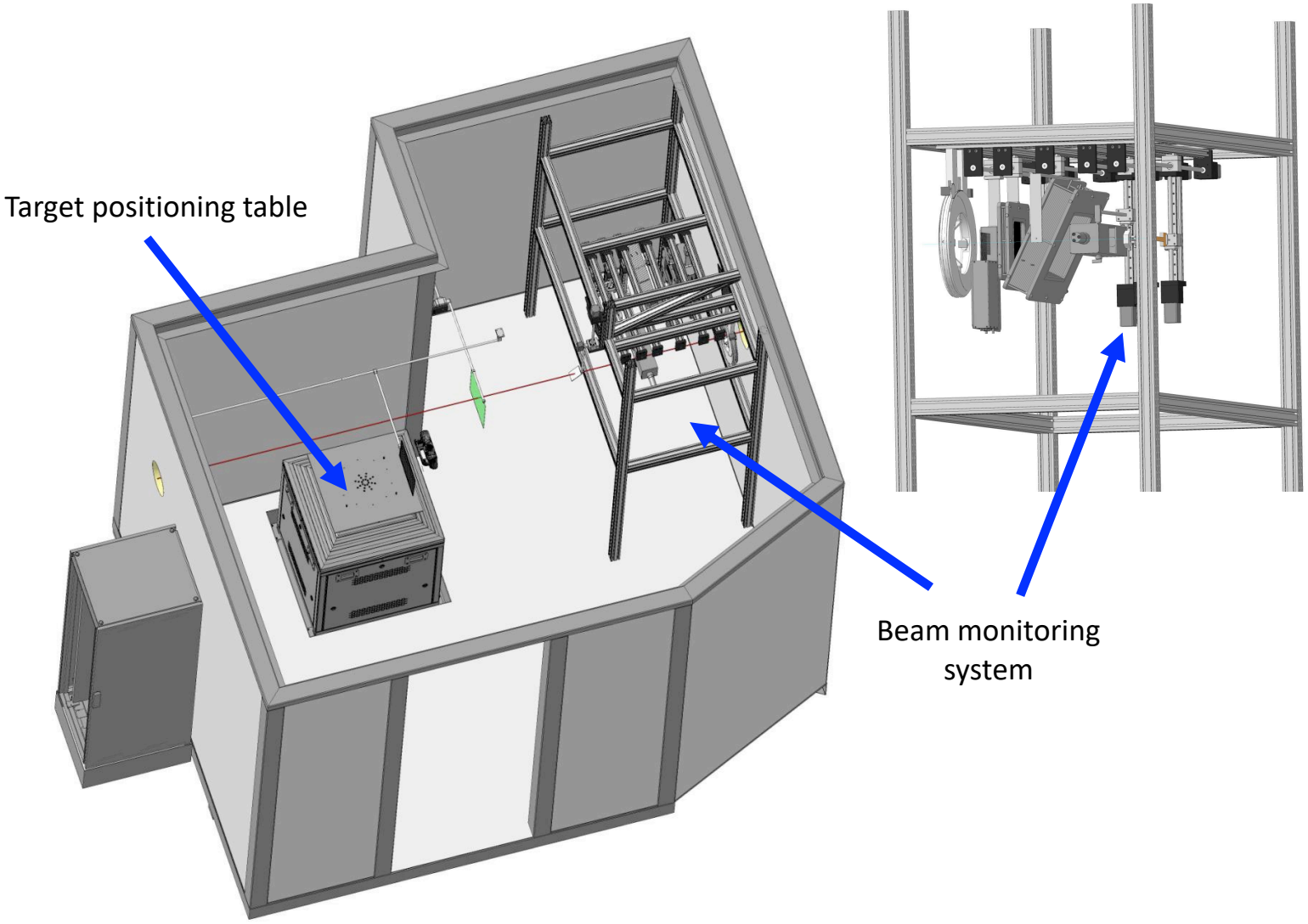

Beam parameters

Ion types	$^{12}C^{6+}$, $^{40}Ar^{18+}$, $^{56}Fe^{26+}$, $^{84}Kr^{36+}$
Ion energy at the exit from the Nuclotron, MeV/n	500-1000
Ion flux density, particles/(cm^2·s)	$10^3..10^6$
Irradiation time per run, min	1-5
Radiation dose, Gy	1-3
Maximum irradiation area in the scanning mode/ nonscanning mode, mm	100x100/Ø10
Flux uniformity for the maximum irradiation area in the scanning mode/ nonscanning mode, %	5/10
Beam FWHM at the target, mm	25-35

The target station is located inside an artificial climate box

E. Syresin et al.

TARGET STATION FOR ADS AND RELATED APPLICATIONS (SHINE)

Area of the target station

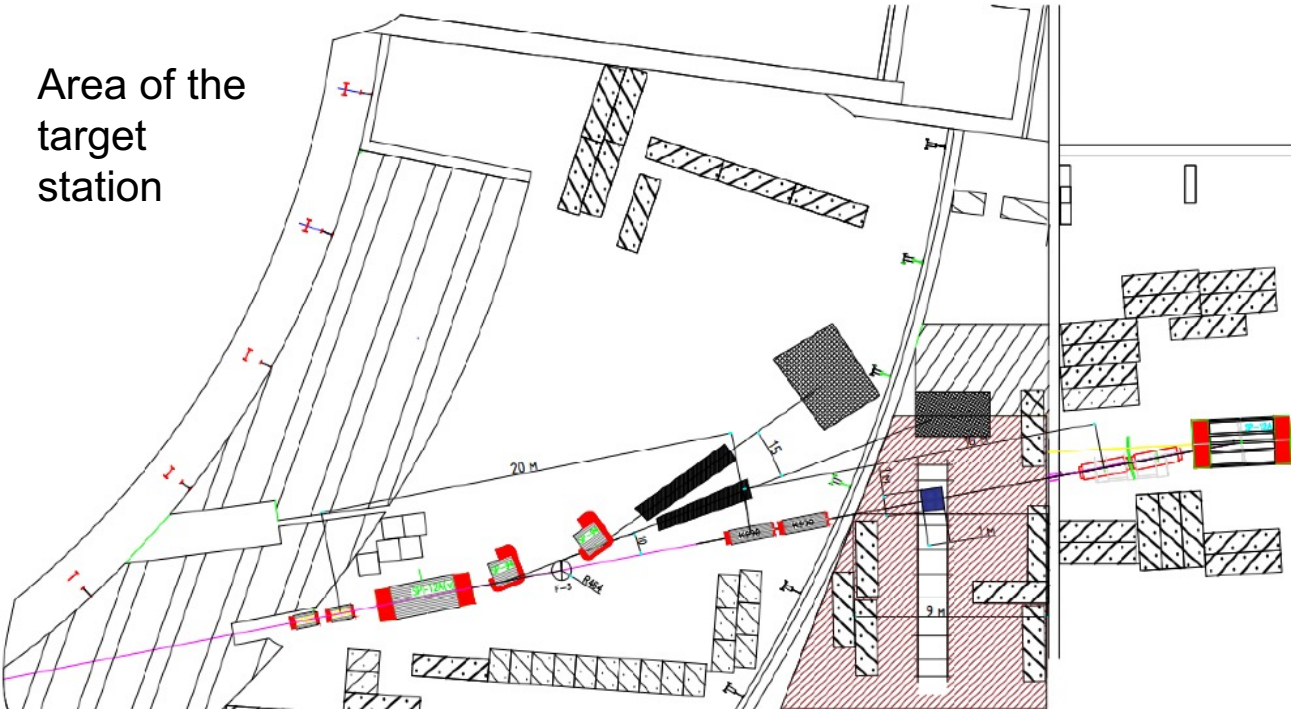

Beam parameters

Ions	$^{12}C^{6+}$, $^{40}Ar^{18+}$, $^{7}Li^{3+}$,$^{1}p^{1+}$, $^{2}D^{1+}$
Ion energy, GeV/n	**0.3-4.0**
Ion intensity, 1/s	$^{1}P^{1+}$, $^{2}D^{1+}$ - 10^{10} $^{12}C^{6+}$, $^{7}Li^{3+}$ - 10^{9}
Nuclear impurities with non goal Z, %	**5**
Field of irradiation, mm	**∅ 20-50**
Fluence at irradiation of a single object	**>10^{14}**

The target station is developed for nuclear power applications and ADS. Light ion beams at energy of 0.3-4 GeV/n are planned to be used for the corresponding research program. Light ions have a short path in the target, which reduces the probability of inelastic nuclear interactions and the required beam power for ADS.

Equipment of the target station involves: targets from C up Pb at length up 1.5 m and diameter up 35 cm, thin targets from Be to U at thickness 0.05-50 mm; beam diagnostic system; target diagnostic system on base of activation and track analysis; target position system; thermometry system; synchronization system; radiation control system; data acquisition system.

A. Baldin et al.

The beams at this target station are also available for other directions of applied research

III. Sample activities and selected results

PILLARS OF APPLIED RESEARCH WITH NICA BEAMS

Radiation effects in microelectronics

Radiation protection in space

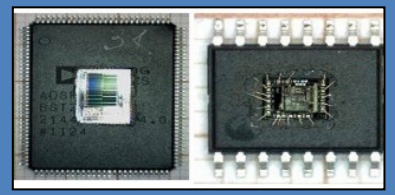

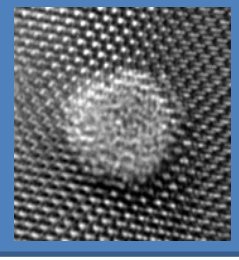

Materials research with ion beams

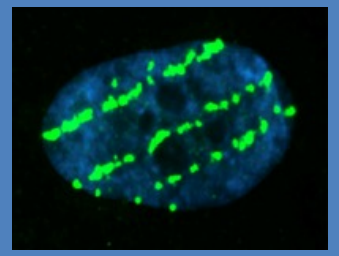

Radiation biophysics and radiobiology

NICA

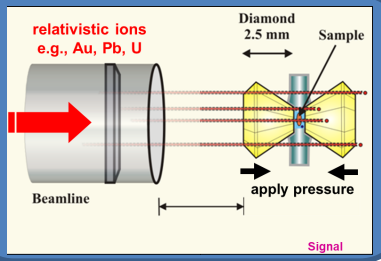

Materials in extreme radiation dose conditions

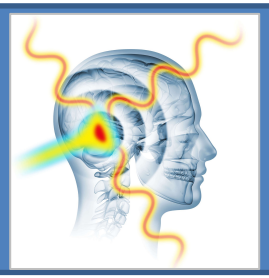

Radiation therapy-related research

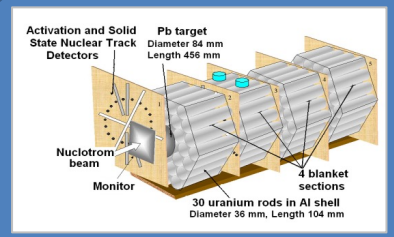

Novel technologies for accelerator-driven systems (ADS)

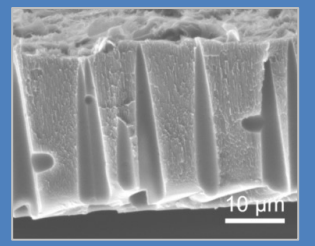

SIMULATION OF SPACE RADIATION COMPONENTS: GALACTIC COSMIC RAYS

Space radiation environment has 2 sources/types

- Galactic Cosmic Rays (GCR) have atomic # 1≤ Z ≤ 92 and energies ~100s of MeV/nucleon and higher (shielding ineffective)
- Solar Particle Events (SPE) have # 1≤ Z ≤ ~26 and energies up to ~10s of MeV/nucleon (shielding can be effective)

Charge

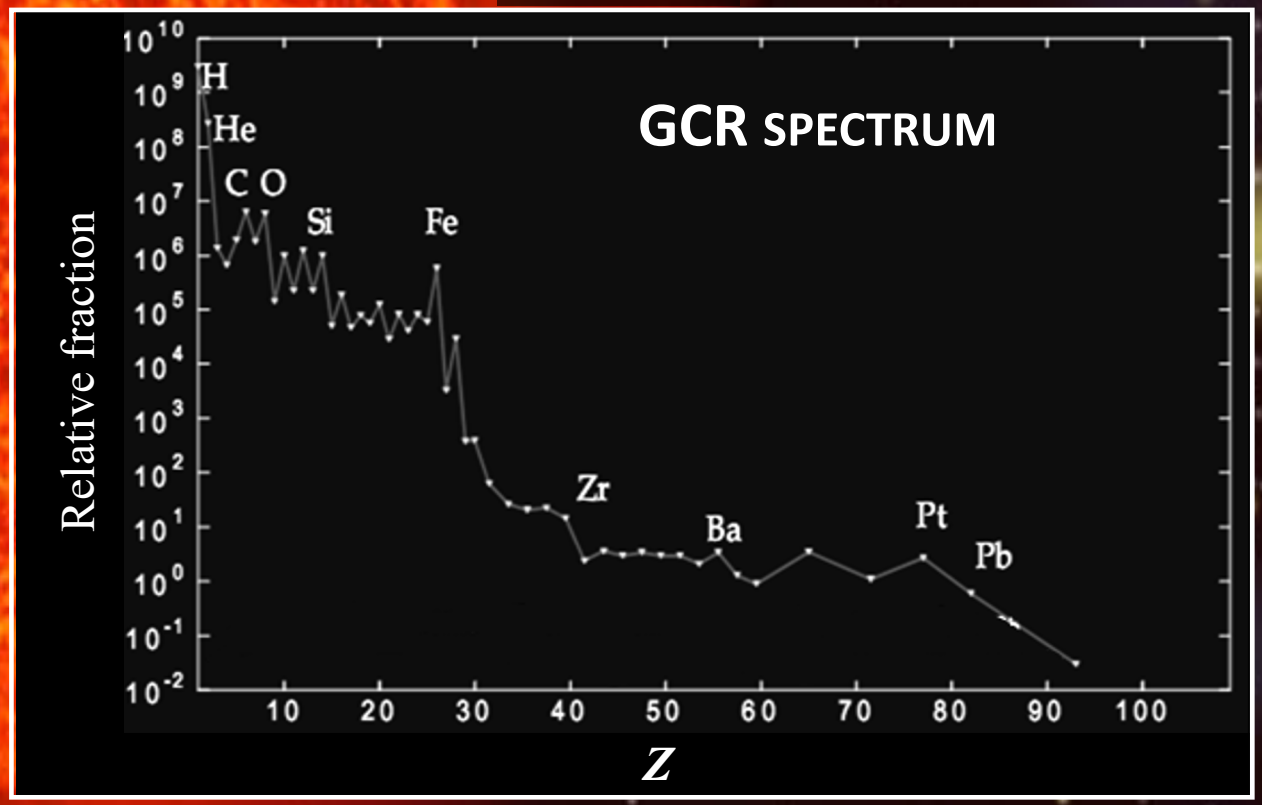

Protons (Z = 1) ~ 92%
He ions (Z = 2) ~ 7%
Ions with c Z = 3÷5 ~ 0.1÷0.15%
Ions of Z = 6÷9 ~ 0,5%
Ions of Z = 10÷15
Ions of Z = 16÷26 ~ 0.065%
Fe ions (Z = 26) ~ 0.025%

Wide range of energies up to 10^{20} eV

/Dorman, 1975;
Kalmykov et al., 2007/

Energy

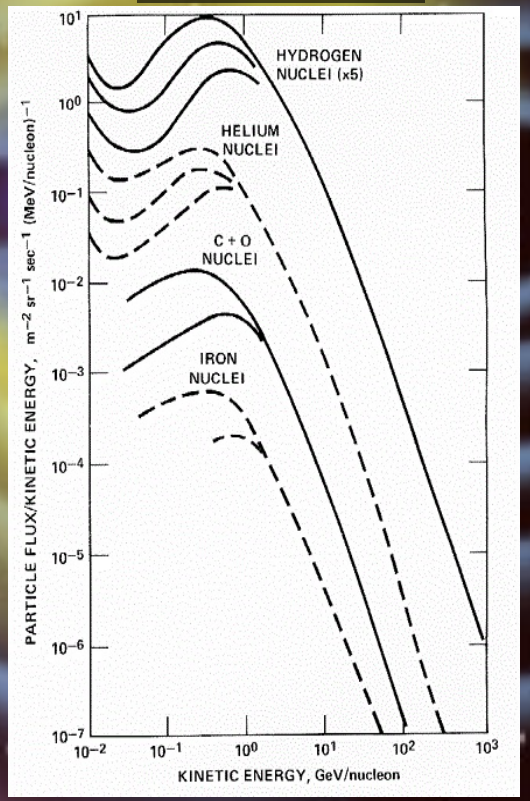

Space Research work package: New composite materials for space industry (protective properties, radiation resistance, radiation-induced modification)

- Improving the regular means of radiation protection in spacecrafts for orbital flights and missions beyond the Earth magnetosphere.
- Study of shielding properties of existing and new composite materials.
- Investigation of radiation modification of composite materials by high-energy accelerated ion beams during long-term irradiation.

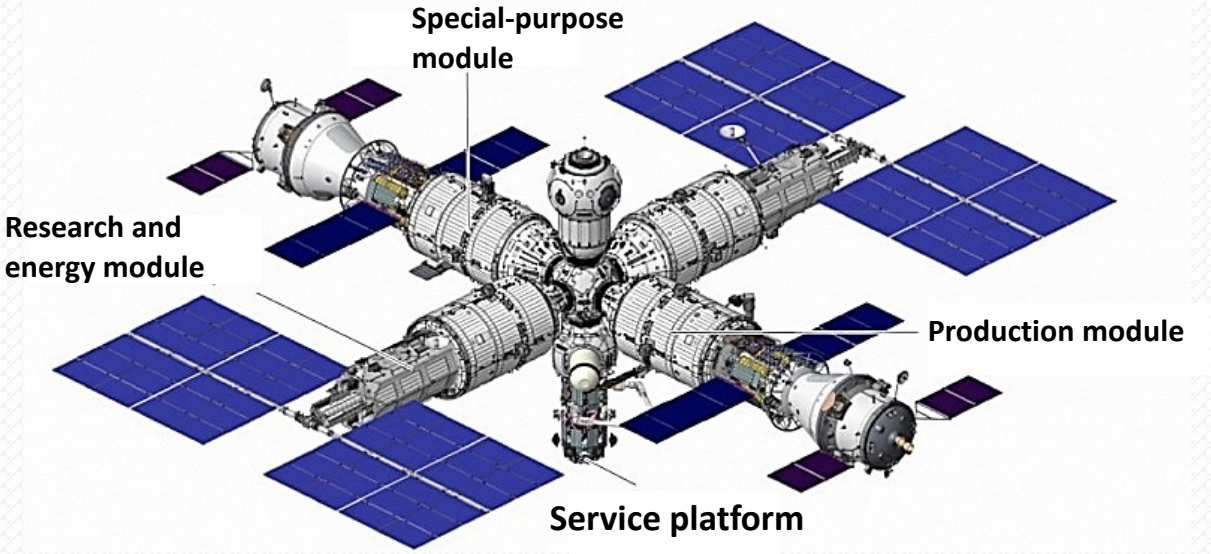

Project of the new Russian Orbital Service Station (ROSS)

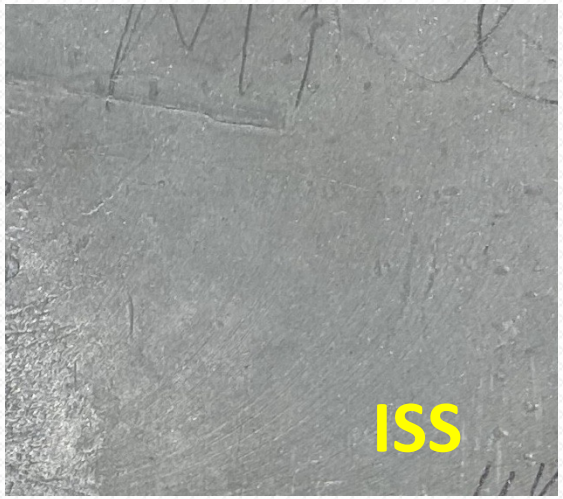

Shielding material from the International Space Station (ISS)

New shielding material for the future Russian Orbital Service Station (ROSS)

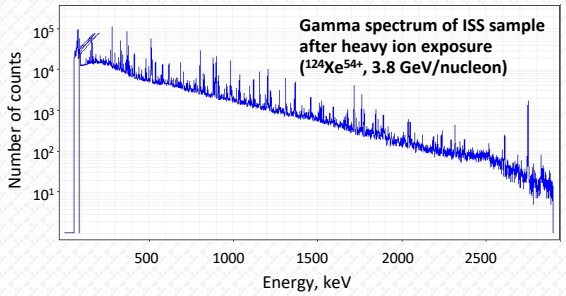

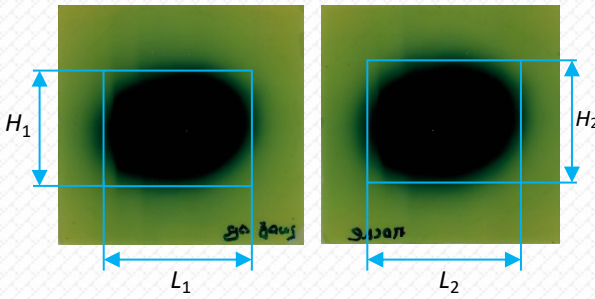

- ❑ Structural, chemico-physical methods of research and testing.
- ❑ Comparative studies under the influence of other types of ionizing radiation.

RADIATION TESTING OF ELECTRONICS WITH IONS OF RELATIVELY HIGH ENERGY

Two types of radiation effects

- Cumulative (dose) effects result from long-term exposure to radiation environment
- Single-Event Effects (SEE) occur promptly due to a **single particle** strike

Recent studies: 25-50% of spacecraft anomalies due to SEE (depends on spacecraft orbits)

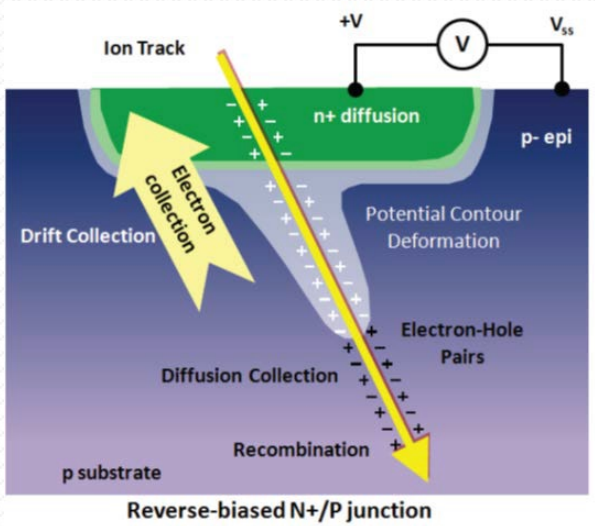

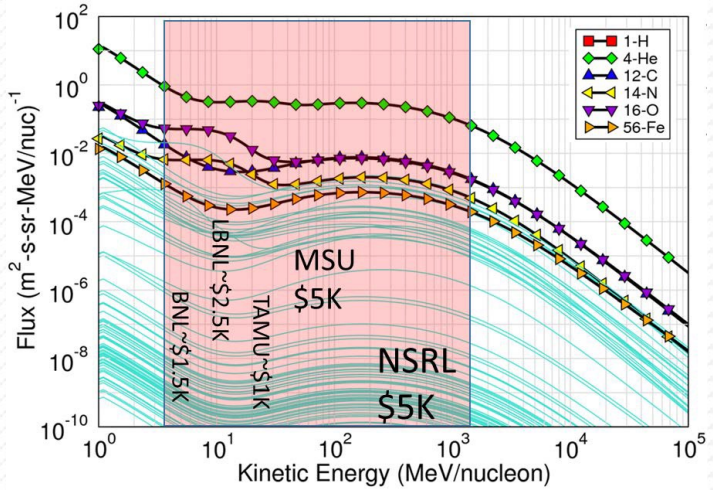

/R.C. Baumann, 2013 NSREC Short Course/

Increasing integration poses problems for SEE testing with low-energy beams

- Multiple die stacked together in packages.
- Behavior may differs if dis-assembled, tested separately.
- Packages now intrinsic to part performance.
- Dis-assembly may compromise timing, thermal and structural characteristics—especially if thinning required.

SEE Frontiers:

1. Technology Frontier
2. Low-Energy Frontier
3. **High-Energy Frontier – relevant to facilities like NICA**

- Ideally, prefer test with ions' characteristic relevant to space
- GCR ions fairly flat out to >2 GeV/nucleon (min. ionizing)
- Difficult and expensive to achieve at accelerators

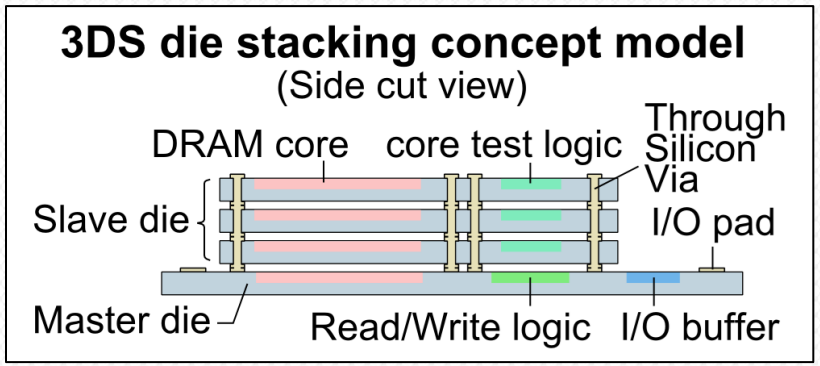

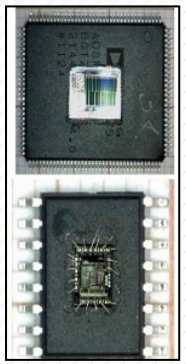

/By R.L. Ladbury at the Meeting of the American Physical Society, Columbus, OH, April 14-17, 2018/

Sample activities of the Life Sciences working package

- Molecular biology research (DNA damage and repair)
- Radiation genetics (gene and structural mutations)
- DNA repair protein biomarkers
- Aspects of the radiation-induced cell death (apoptosis, necrosis)
- Formation of chromosomal aberrations
- Different aspects of radiation-induced cancerogenesis
- Central nervous system disorders following the radiation exposure
- Development of radiation protection measures
- Improvement of beam delivery and dosimetry methods for radiotherapy
- …

DNA REPAIR PROTEIN MARKERS FOR CANCER CHARACTERIZATION

Studying the mechanisms and regularities of DNA repair in normal and cancer cells exposed to different types of radiation exposure (including ion beams produced by NICA facility) enables to identify specific protein markers associated with cancer.

RADIATION-INDUCED DNA DAMAGE

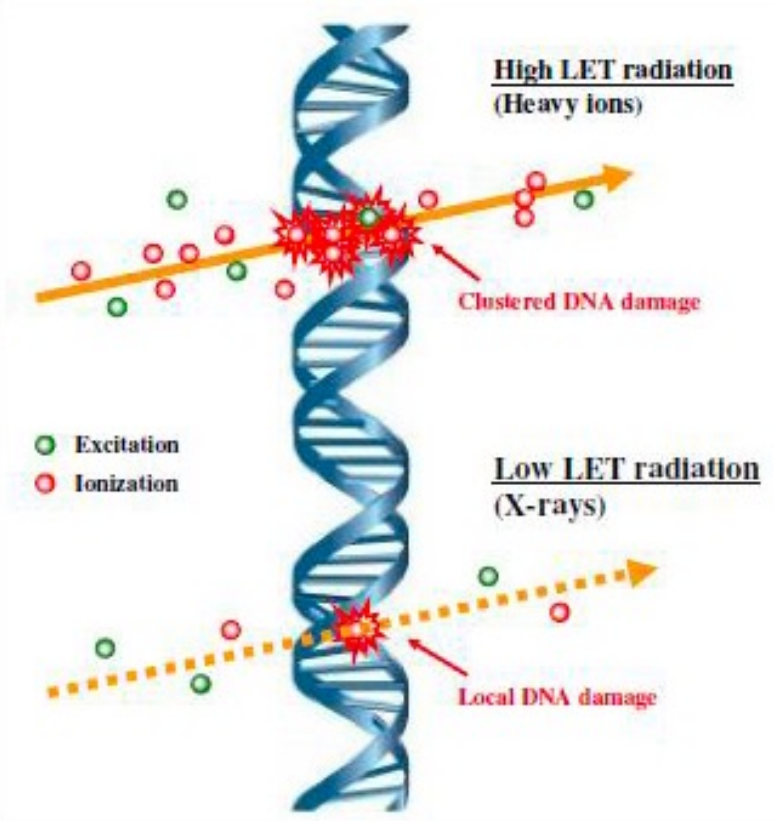

Modified from W. Tinganelli and M. Durante. Carbon Ion Radiobiology. Cancers 2020, 12, 3022

DNA DOUBLE-STRAND BREAK REPAIR

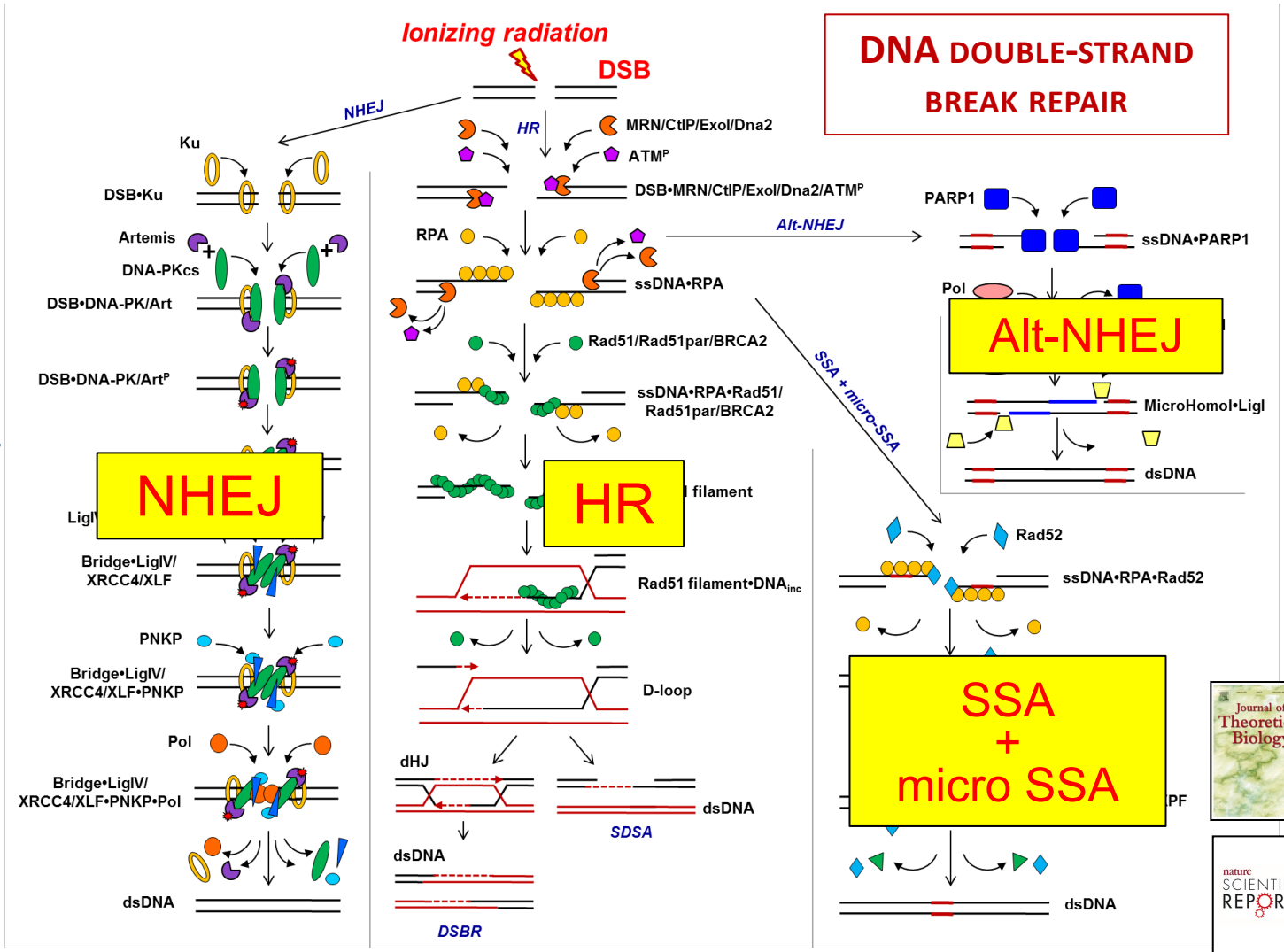

Modified from O. Belov et al., 2015–2023

DNA REPAIR PROTEIN MARKERS FOR BREAST CANCER CHARACTERIZATION

An example is the characterization of the ***triple-negative breast cancer (TNBC)*** being a kind of breast cancer that does not have any of the receptors that are commonly found in this type of cancer. It is estrogen receptor (ER) negative, progesterone receptor (PR) negative and HER-2 low by immunohistochemistry or fluorescent in-situ hybridization.

The characterization method is based on determining the levels of several DNA repair proteins using specific antibodies against proteins in multiple DNA repair pathways. Possible set of antibodies :

XPF — nucleotide excision repair (NER),
FANCD2 — Fanconi Anemia/homologous recombination (FA/HR),
MLH1 — mismatch repair (MMR),
pMK2 — MAPKAPKinase2, DNA damage response (DDR).

The DNA repair patterns exhibiting low XPF, pMK2, MLH and FANCD2 can be associated with shorter time to recurrence of the breast cancer.

A 4-antibody model is suggested to be able to segregate high risk and low risk groups based on time to recurrence of TNBC.

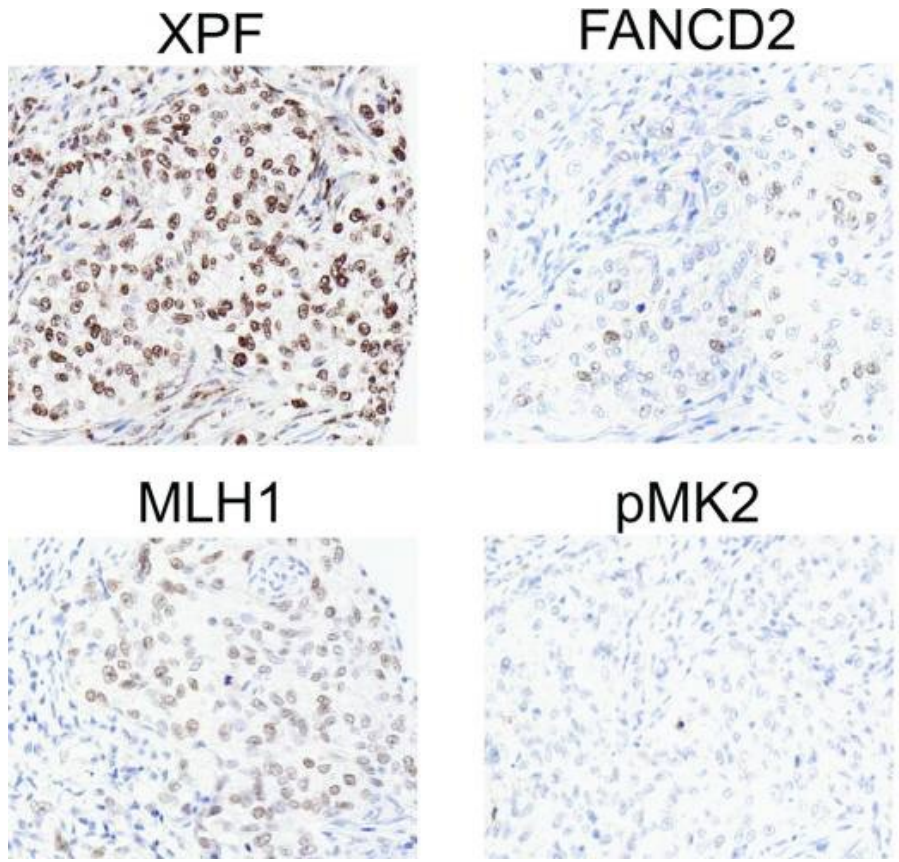

Immunohistochemistry patterns for the several DNA repair antibodies in one triple negative breast tumor

Alexander et al. Clin Cancer Res. 2010; 16(23):5796-804

SEEKING FOR OVERALL PATTERNS OF DNA REPAIR IN DIFFERENT CANCER CELLS FOR FURTHER USE IN PREDICTION AND DIAGNOSTICS

Defining the DNA repair patterns both in its native form and following the exposure to ionizing radiation

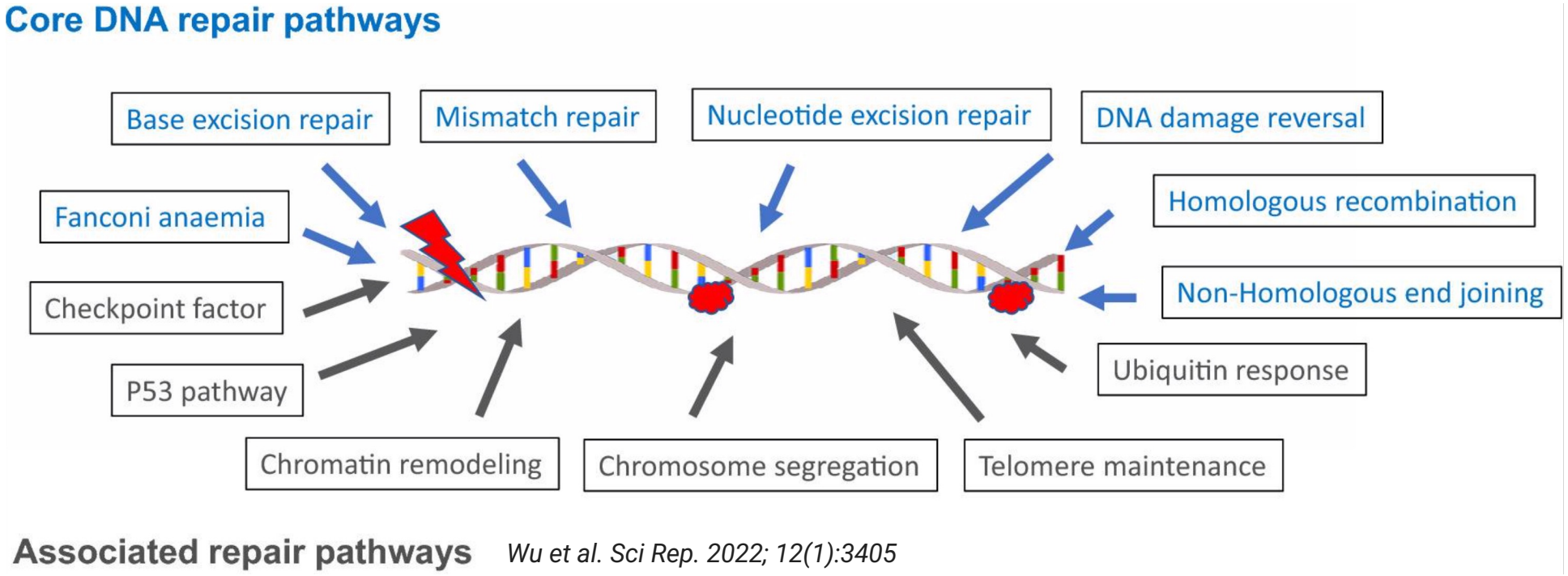

Wu et al. Sci Rep. 2022; 12(1):3405

STUDY OF BEHAVIORAL AND NEUROCHEMICAL OUTCOMES IN LABORATORY ANIMALS FOLLOWING APPLICATION OF CHEMICAL AND/OR RADIATION FACTORS

(Both for space-related research and for or preclinical studies using animals to investigate the potential of a therapeutic drug or strategy)

Probing the variety of behavioral reactions in laboratory animals following application of chemical and/or radiation factors:

- **anxiolytic-/anxiogenic-like effects;**
- **sedative effects;**
- **depression model;**
- **locomotor activity;**
- **memory;**
- **stress-vulnerability, etc.**

Application of behavioral test sets:

- Open Field;
- Elevated Plus Maze;
- Rotarod Performance Test;
- Passive Avoidance Task;
- etc.

Belov et al., 2015-2022

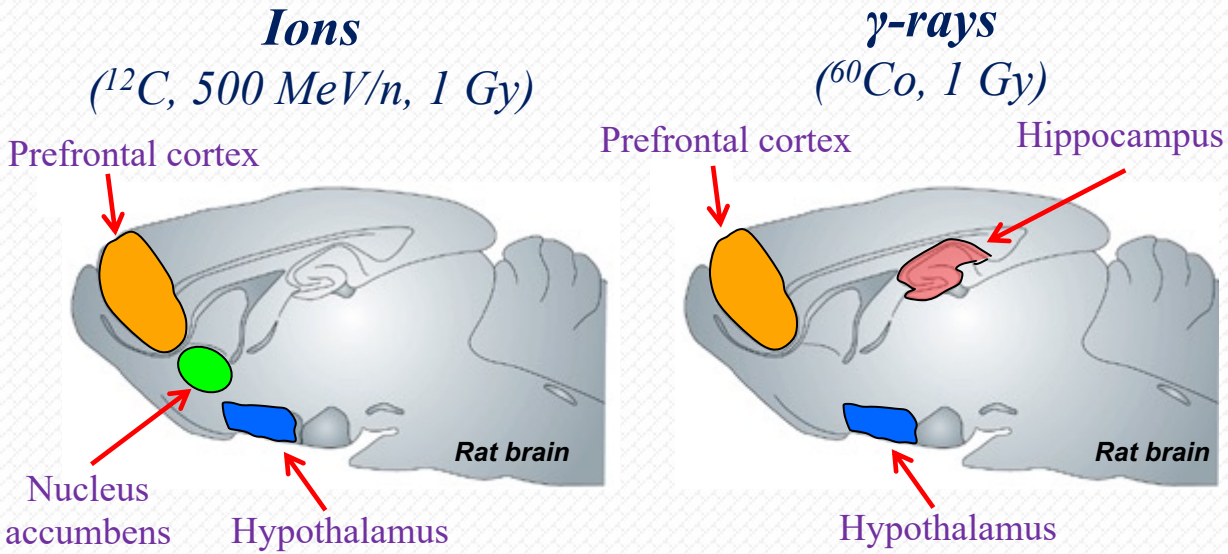

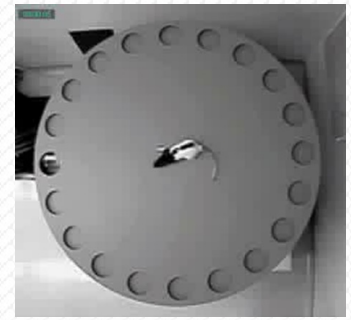

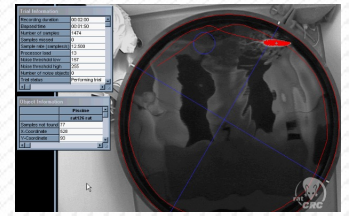

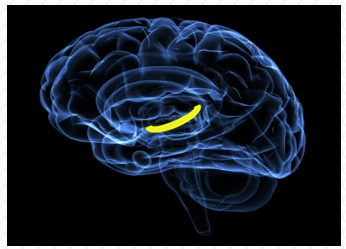

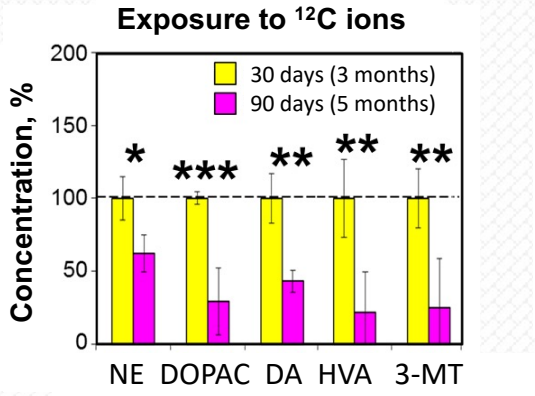

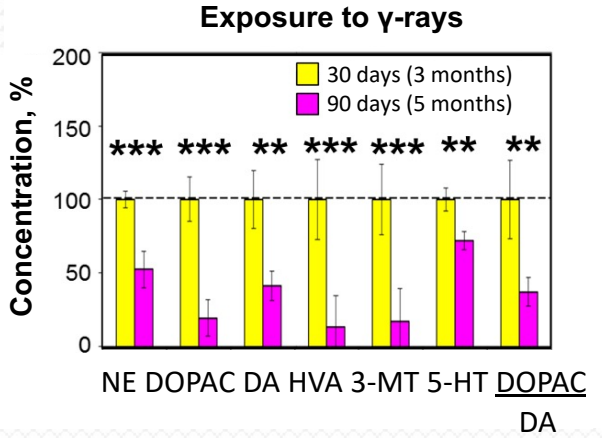

Seeking for most radiosensitive brain structures

STUDY OF RADIOLYTIC DAMAGE TO NEURAL CELL STRUCTURES

DISTRIBUTION OF FREE RADICALS IN A SINGLE PYRAMIDAL NEURON AFTER IRRADIATION

30 MeV $^{+}$p particle track →

1000 MeV/u ^{56}Fe particle track →

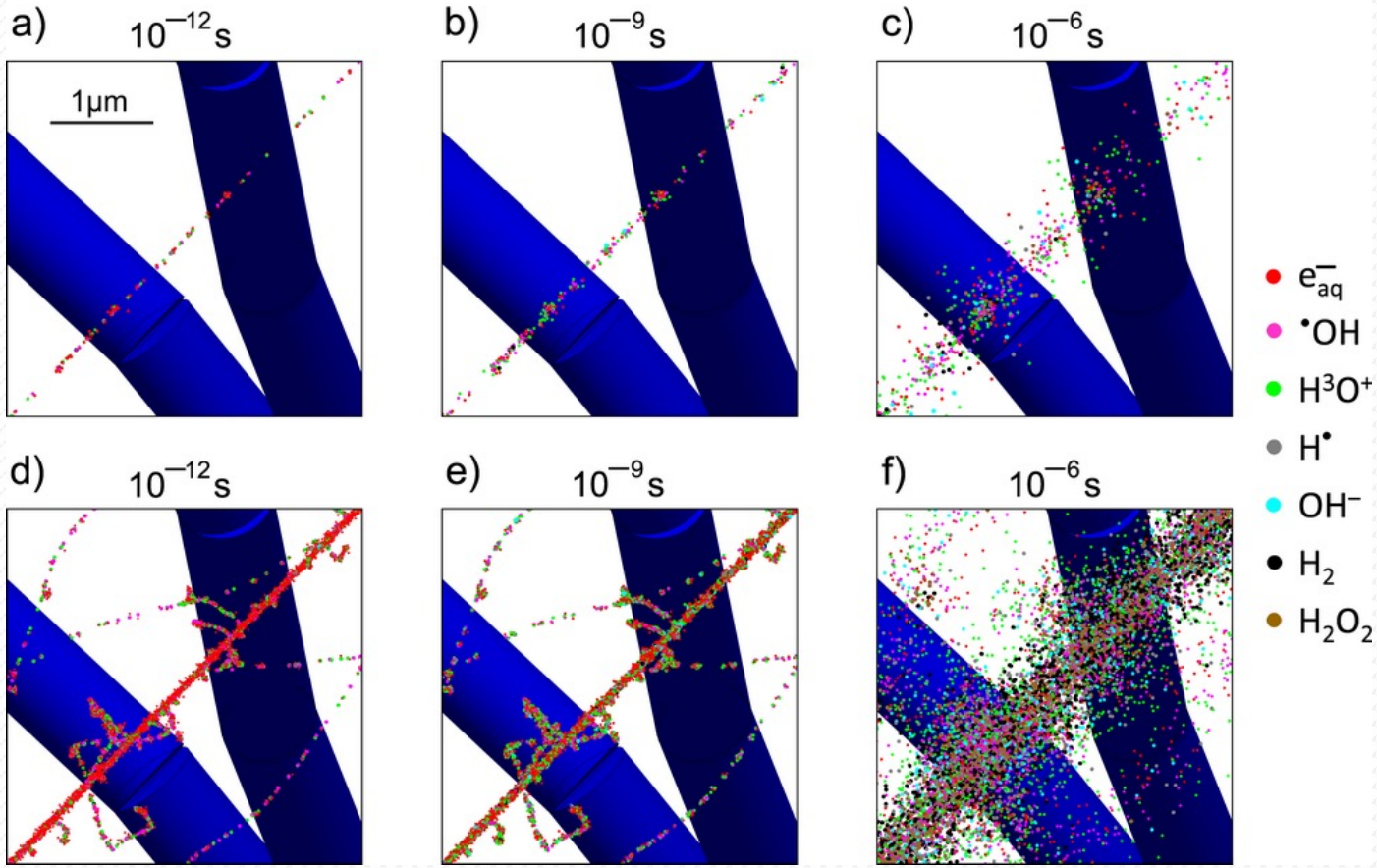

Experimental verification is needed!

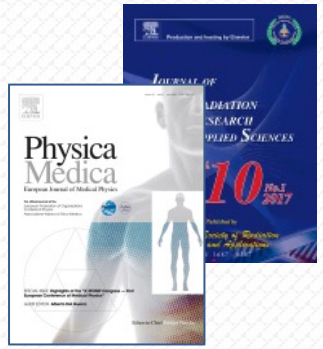

Track structure of a 30 MeV proton and 1000 MeV/u ^{56}Fe ion in dendritic branches of pyramidal neuron, as viewed at picosecond, nanosecond, and microsecond after exposure

Belov et al., 2019-2021

RADIATION PROTECTION FRONTIER

Development and testing of pharmaceuticals for protecting astronauts from space radiation on experimental models of laboratory animals

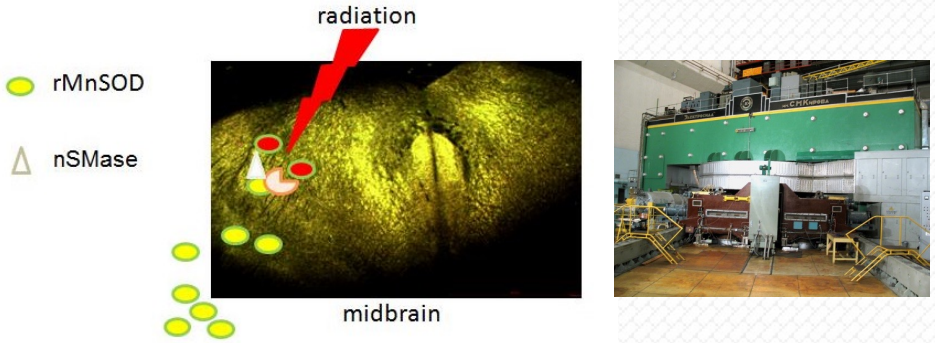

It has been established that recombinant human manganese-containing superoxide dismutase (rMnSOD), which has specific antioxidant and antiradical activity, is able to overcome the blood-brain barrier and penetrate into the midbrain, preventing radiation damage.

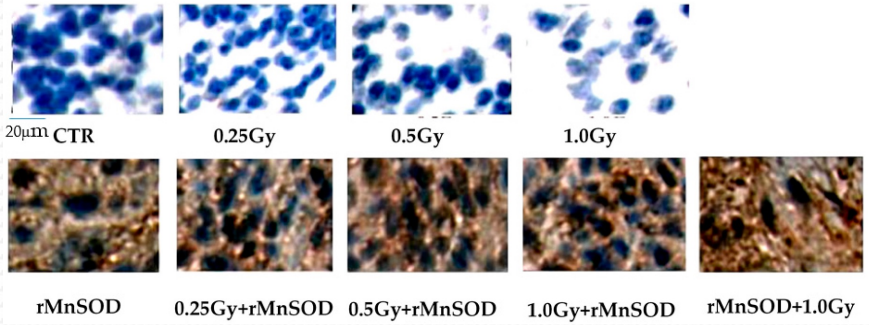

Localization of rMnSOD in brain tissue. Immunohistochemical analysis was performed by using specific antibody. The immunostaining was evident only in brain samples from rMnSOD-treated mice.

Cataldi, S.; Borrelli, A.; Ceccarini, M.R.; Nakashidze, I.; Codini, M.; Belov, O.; Ivanov, A., et al. Neutral Sphingomyelinase Modulation in the Protective/Preventive Role of rMnSOD from Radiation-Induced Damage in the Brain. Int. J. Mol. Sci. 2019, 20, 5431.

The ability of rMnSOD to reduce radiation-induced damage has been shown, both through a protective role associated with sphingomyelinase with an acidic pH optimum (aSMase), and through a prophylactic role through sphingomyelinase with a neutral pH optimum (nSMase).

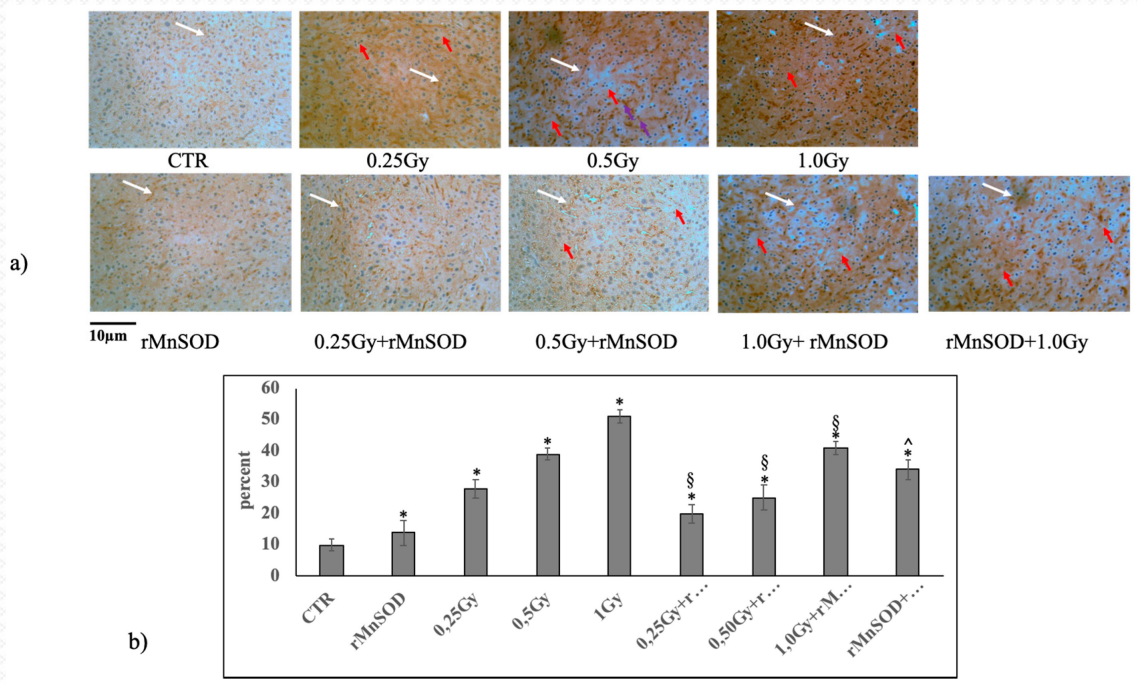

Mouse liver after irradiation with or without protective or preventive rMnSOD treatment (**a**) representative liver histology by Caspase-1 immunohistochemical staining. (**b**) Quantification of Caspase-1 staining was performed using the ImageFocus software. Positive staining is indicated as low (+), medium (++), or high (+++). Only high positive staining was considered and was measured as a percentage of the total area. Data represent the mean + S.D. of three livers for each group. Significance, * $p < 0.05$ with respect to the CTR, § $p < 0.05$ with respect to the irradiated samples, ^ $p < 0.05$ with respect to 1.0 Gy + rMnSOD.

Cataldi S, Borrelli A, Ceccarini MR, Nakashidze I, Codini M, Belov O, Ivanov A, et al. Acid and Neutral Sphingomyelinase Behavior in Radiation-Induced Liver Pyroptosis and in the Protective/Preventive Role of rMnSOD. Int J Mol Sci. 2020, 21(9), 3281.

Materials Science working package: Irradiation of high-temperature superconducting tapes

- Development of methods for increasing the critical current of high-temperature superconductors (HTSC) by means of radiation modification (induction of pinning centers in the bulk of the superconductor).
- Comparative analysis of the critical current values upon irradiation of HTSC tapes with $^{124}Xe^{54+}$ ions of 3.8 GeV/nucleon and protons of 660 MeV.
- Estimation of the stability of the effect of increasing the critical current in an irradiated superconductor.
- Development of equipment prototypes based on radiation-modified HTSC tapes and their testing.

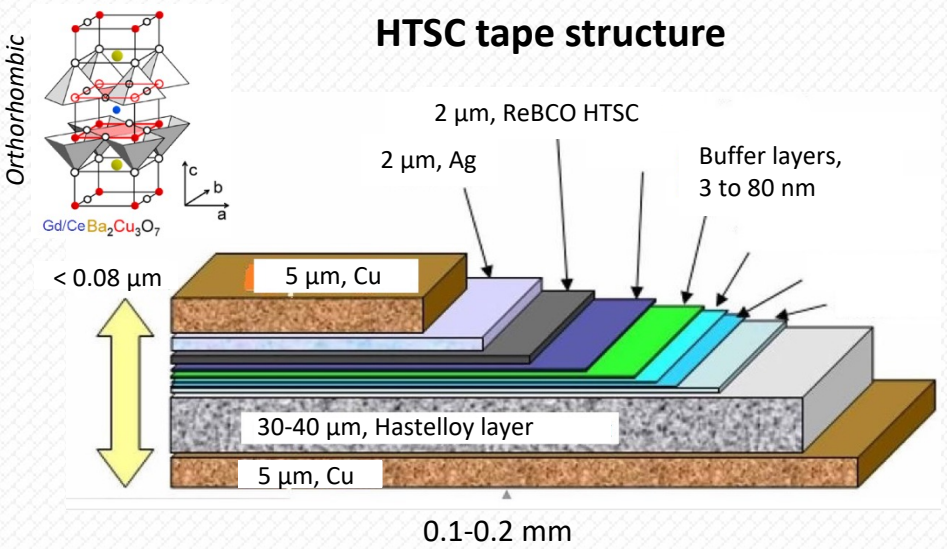

Methods for measuring current-voltage characteristics, Hall coefficient, magnetoresistance, thermo-EMF coefficient, thermal conductivity coefficient, magnetic moment in the temperature range of 1.7–300 K and magnetic fields up to 8 T.

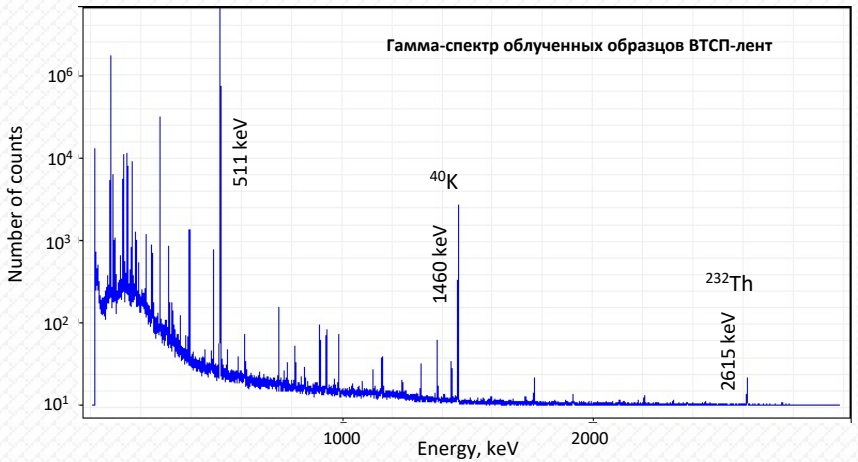

Irradiation of vertically and horizontally arranged HTSC tapes with and without copper content

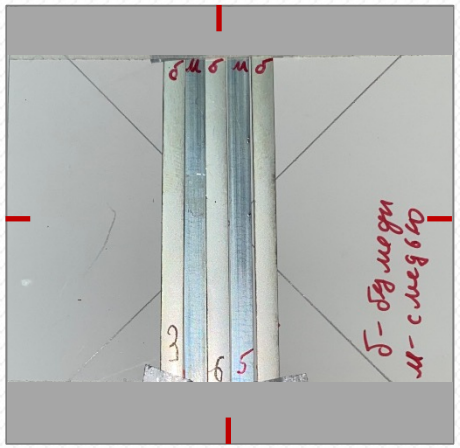

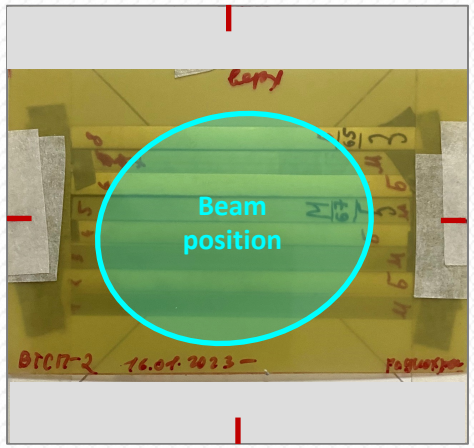

Radiation modification of polytetrafluoroethylene (PTFE), polyethylene terephthalate (PET), polyethylene (PE) and polyimide (PI) films

- Study of the processes of amorphization and recrystallization of polymers and nanocomposite materials.
- Investigation of regularities of radiation-chemical damages in PTFE, PET, PE and PI films.
- Establishment of regularities in radiolysis of condensed matter under the exposure to ion beams with energies of several GeV/nucleon.
- Development of ion-track technologies with "thick" targets and multilayer materials.

Multilayer film packs for exposure

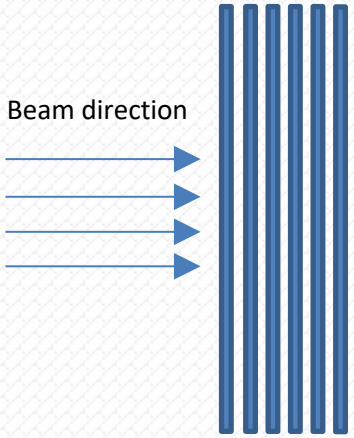

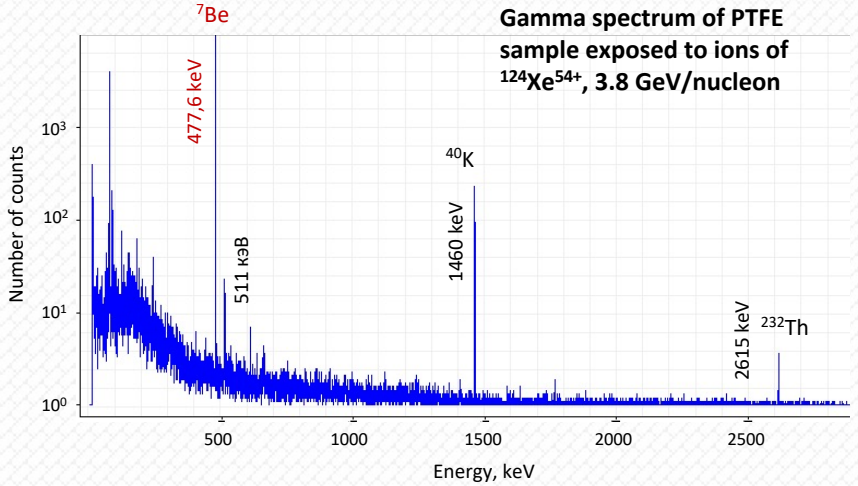

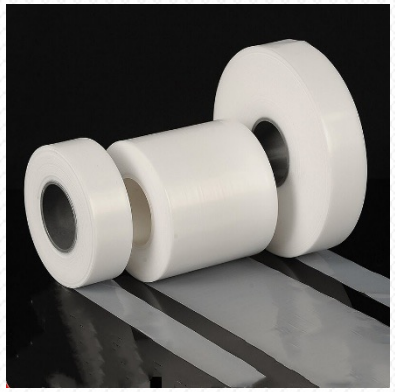


PTFE, PET, PE and PI films of 12, 20, 40, 50, 80 µm thick

Research methods: scanning and transmission electron microscopy, X-ray phase analysis, X-ray photoelectron spectroscopy and X-ray energy-dispersive elemental analysis, atomic force microscopy and low-temperature nitrogen sorption, wettability with respect to water and heptane, optical and infrared spectroscopy, infrared spectroscopy of frustrated total internal reflection, diffuse spectroscopy and specular reflection, laser Doppler strainmetry.

STUDY OF RADIATION MODIFICATIONS IN SAPPHIRES (Al_2O_3) AS A RESULT OF THE LONG-TERM HEAVY ION EXPOSURE

Study of structural modifications and the state of matter as a result of the accelerated ion beam exposure of on sapphires (Al_2O_3).

Improvement of the "silicon on sapphire" technology in topics assuming the impact of relatively high-energy ions (deep space, radiation-resistant electronics for charged particle accelerators, etc.).

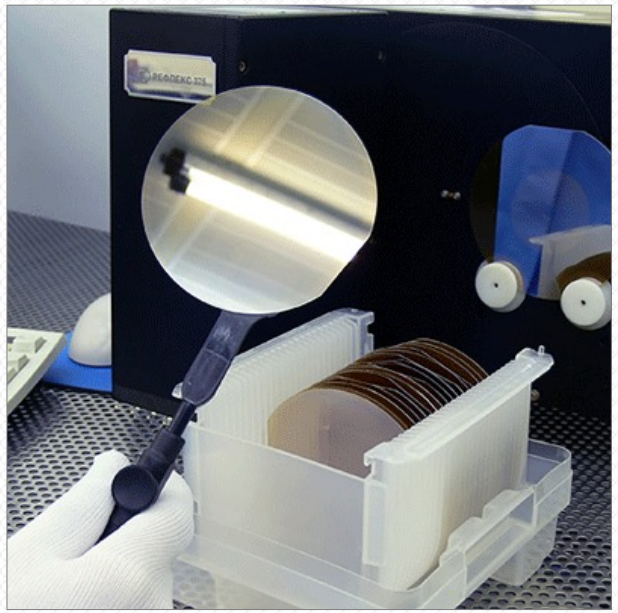

Research methods used:
atomic force microscopy; scanning electron microscopy; electron spectroscopy for chemical analysis; X-ray fluorescence analysis; mass spectrometry; thermal analysis.

Samples of sapphires*

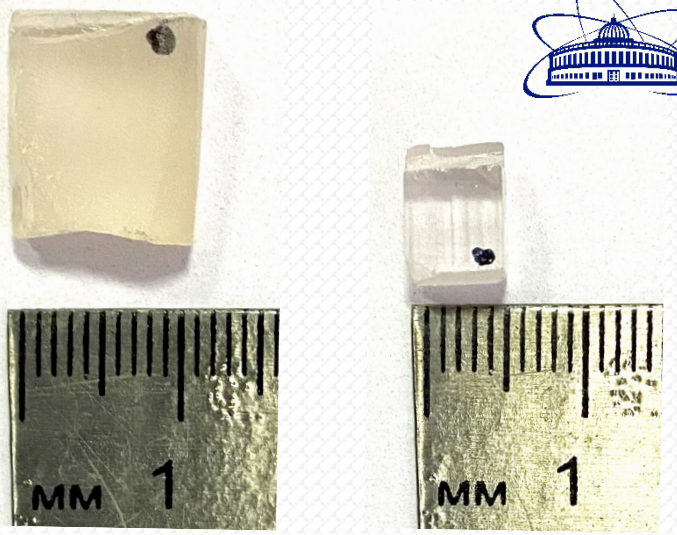

*Transparent wedge-shaped samples of crystalline alumina (sapphire) produced by the Vernel method.

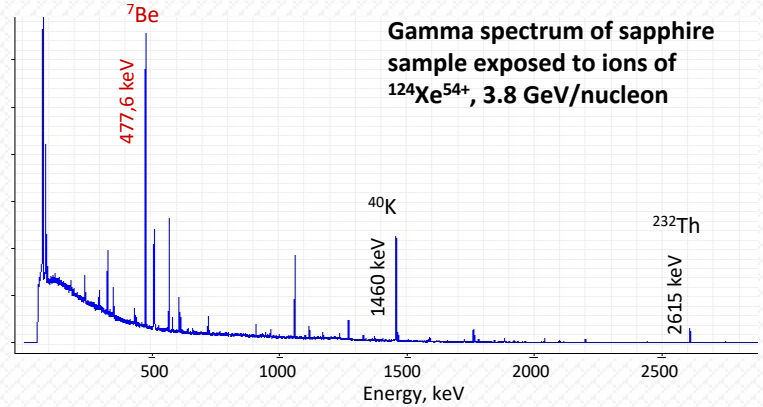

NOVEL NUCLEAR TECHNOLOGIES WITH NICA BEAMS

Accelerator Driven Systems (ADS) are the nuclear systems based on interaction of particle beams extracted from the accelerator with deeply subcritical quasy-infinite active zones consisting of the depleted (natural) uranium, thorium and spent nuclear fuel.

In previous years, the conditions which maximize the efficiency of ADSR were investigated. The optimal value of criticality coefficient of the core k_{eff} is in the range 0.985 - 0.988. It was suggested that the best choice for the converter is Be, especially for ion beams at low energy.

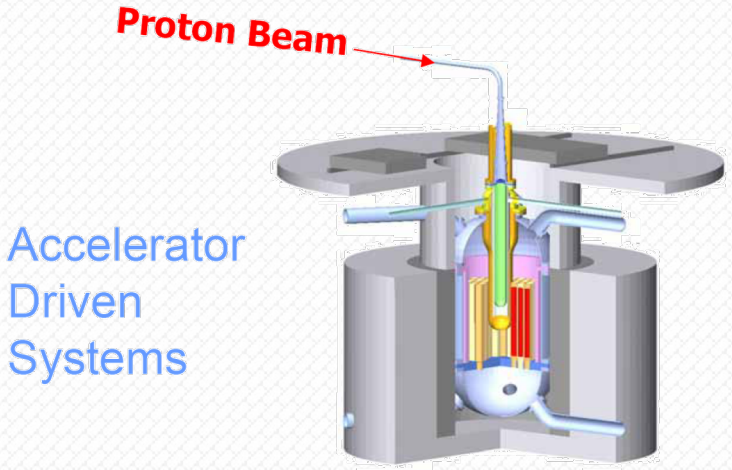

The maximum energy gain of protons is obtained at 1.5 GeV when they are accelerated in a LINAC, and at lower energy (0.75-1 GeV) when a cyclotron is used. In both situations ion beams starting with ^{4}He realize higher energy gain than protons. When particles are accelerated in a LINAC, at low accelerator length a beam of ^{7}Li with energy 0.25 AGeV represents the best option.

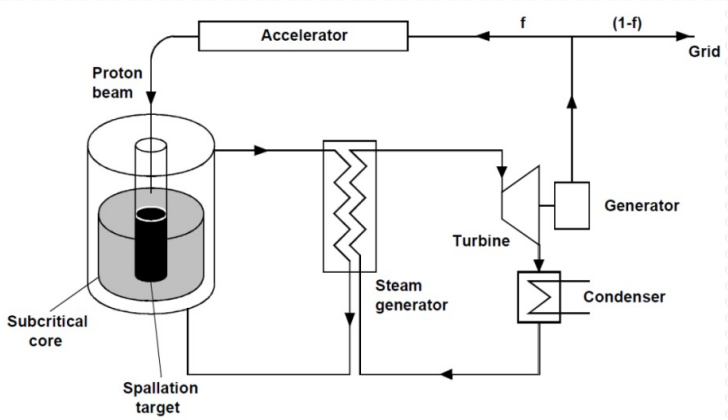

Within the next years the ADSR project will be concentrated on:

- **Research activities, involving simulation study, on an optimal design of the target;**
- **Verification of a principally new concept of a system based on the use of ion beams instead of protons;**
- **Implementation of the first stage of experimental program focused on measurement of the neutron yields with different converter combinations.**

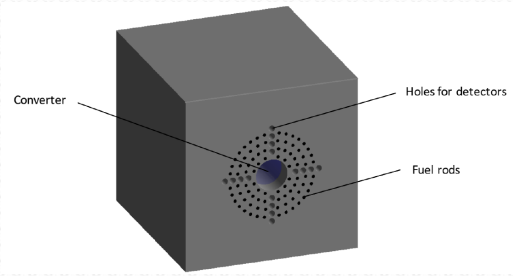

IV. Ways to be involved in the ARIADNA collaboration on applied research at NICA

ARIADNA COLLABORATIONS FOR APPLIED RESEARCH AT NICA

ARIADNA-LS Collaboration	ARIADNA-MSTE Collaboration	ARIADNA-NPT Collaboration
The Collaboration is being established in order to perform experiments in the field of life sciences at the NICA Complex with the ARIADNA beamlines	The Collaboration is being established in order to perform activities and experiments in radiation materials science and radiation testing of electronics at the NICA Complex with the ARIADNA beamlines	The Collaboration is being established in order to facilitate novel developments for nuclear technology at the NICA Complex with the ARIADNA beamlines

Collaborating organizations

1. Joint Institute for Nuclear Research (Dubna, Int.)
2. Institute of Biomedical Problems, RAS (Moscow, Russia)
3. Burnasyan Federal Medical Biophysical Center of Federal Medical Biological Agency (Moscow, Russia)
4. Skobeltsyn Research Institute of Nuclear Physics, Moscow State University (Dubna, Russia)
5. Saint Petersburg State University (Saint Petersburg, Russia)
6. Tsyb Medical Radiological Research Centre (Obninsk, Russia)
7. Semenov Research Center of Chemical Physics, RAS (Moscow, Russia)
8. Institute of Theoretical and Experimental Biophysics, RAS (Moscow, Russia)
9. Moscow Institute of Physics and Technology (Dolgoprudny, Russia)
10. Kurnakov Institute of General and Inorganic Chemistry, RAS (Moscow, Russia)
11. National Research Nuclear University MEPhI (Moscow, Russia)
12. Joint Institute of High Temperatures, RAS (Moscow, Russia)
13. North Ossetian State University (Vladikavkaz, Russia)
14. Institute of Nuclear Problems of the Belarusian State University (Minsk, Belarus)
15. LLC Research and production company “Kvant-R” (Moscow, Russia)
16. LLC “S-Innovations” (Moscow, Russia)
17. LLC “SOL-Instruments” (Minsk, Belarus)
18. IC CANDLE, Yerevan, Armenia
19. Yerevan State University, Yerevan, Armenia

157 participants

ARIADNA ACCESS

- Both academic and industrial groups are eligible to access the ARIADNA infrastructure.
- A correspondingng user policy at NICA is under development, which includes regulations on equipment use, bioethics, access to beamlines and to supportive user infrastructure, etc.
- Funding opportunities can also be provided on the basis of special-purpose grant programs launched for NICA by external funding agencies.
- Main counterpart from ARIADNA users: results need to be published!

WAYS OF GETTING INVOLVED IN ARIADNA

- As a **member of ARIADNA collaboration:** get in touch with us and we will provided instructions on signing an MoU to become a member of the collaboration.
- As a **user:** just prepare and submit you proposal for consideration.
- As an **ARIADNA partner:** let us know how you think you/your research team or company can contribute to ARIADNA and we can prepare a relevant application to be discussed with NICA management.

THANK YOU FOR YOUR ATTENTION